AD_____

Award Number: W81XWH-09-1-0064

TITLE: Dynamic Testing of Signal Transduction Deregulation During Breast Cancer Initiation

PRINCIPAL INVESTIGATOR: Tuan Vo-Dinh, Ph.D.

CONTRACTING ORGANIZATION: Duke University
Durham, NC 27708

REPORT DATE: July 2011

TYPE OF REPORT: Final

PREPARED FOR: U.S. Army Medical Research and Materiel Command
Fort Detrick, Maryland 21702-5012

# REPORT DOCUMENTATION PAGE

*Form Approved*
*OMB No. 0704-0188*



| 1. REPORT DATE | 2. REPORT TYPE | 3. DATES COVERED |
|---|---|---|
| July 2011 | Final | 1 July 2009 – 30 June 2011 |

**4. TITLE AND SUBTITLE**

Dynamic Testing of Signal Transduction Deregulation During Breast Cancer Initiation

**5a. CONTRACT NUMBER**

**5b. GRANT NUMBER**
W81XWH-09-1-0064

**5c. PROGRAM ELEMENT NUMBER**

**6. AUTHOR(S)**

Tuan Vo-Dinh (PI), Victoria Seewaldt (co-PI), Yan Zhang, Jonathan P. Scaffidi, Molly K. Gregas, Benoit Lauly, Stephen DeVience, Anuj Dhawan, Hsinneng Wang, Hsiang-Kuo Yuan, Chris Khoury
E-Mail: tuan.vodinh@duke.edu

**5d. PROJECT NUMBER**

**5e. TASK NUMBER**

**5f. WORK UNIT NUMBER**

**7. PERFORMING ORGANIZATION NAME(S) AND ADDRESS(ES)**

Duke University
Durham, MC 27708

**8. PERFORMING ORGANIZATION REPORT NUMBER**

**9. SPONSORING / MONITORING AGENCY NAME(S) AND ADDRESS(ES)**
U.S. Army Medical Research and Materiel Command
Fort Detrick, Maryland 21702-5012

**10. SPONSOR/MONITOR'S ACRONYM(S)**

**11. SPONSOR/MONITOR'S REPORT NUMBER(S)**

**12. DISTRIBUTION / AVAILABILITY STATEMENT**
Approved for Public Release; Distribution Unlimited

**13. SUPPLEMENTARY NOTES**

**14. ABSTRACT**
The goal of our study is to develop nanosensors to detect pre-cancerous changes in the breast and figure out which pre-cancerous breast changes have the highest chance of progressing to become invasive breast cancer. In particular, we are developing targeted nanobiosensors to test real-time protein phosphorylation signaling in live RPFNA cells. In this study, we have designed fiber-optic nanoprobes for optical detection in single living cells. The nanoprobes were fabricated with well-controlled nanoapertures for optimized spatial resolution and optical transmission. The nanoprobes were characterized with scanning electron microscopy and near-field scanning optical microscopy to ensure optimal performance. Theoretical analysis determined the probing depth and volume of the nanoprobe. The nanoprobes have been demonstrated for detection of biologically significant species in single living cells. The nanobiosensors allow us to directly test for complex protein changes in breast cells taken from high-risk women.

**15. SUBJECT TERMS**
Fiber-optic nanoprobe; single-cell analysis

| 16. SECURITY CLASSIFICATION OF: | | | 17. LIMITATION OF ABSTRACT | 18. NUMBER OF PAGES | 19a. NAME OF RESPONSIBLE PERSON |
|---|---|---|---|---|---|
| a. REPORT | b. ABSTRACT | c. THIS PAGE | | | USAMRMC |
| U | U | U | UU | 31 | 19b. TELEPHONE NUMBER *(include area code)* |

# Table of Contents

## INTRODUCTION:

The goal of this study is to develop nanosensors to detect pre-cancerous changes in the breast and figure out which pre-cancerous breast changes have the highest chance of progressing to become invasive breast cancer. In particular, we are developing targeted nanobiosensors to test real-time signaling in live RPFNA cells. In this study, we have designed and fabricated fiber-optic nanoprobes for optical detection in single living cells from breast cancer patient. The nanoprobes were fabricated with well-controlled nanoapertures for optimal spatial resolution and optical transmission. The nanoprobes were characterized with scanning electron microscope and near-field scanning optical microscope. Theoretical analysis determined the probing depth and volume of the nanoprobe. The nanoprobes have been demonstrated for detection of biologically significant species in single living cells.

## BODY:

There is a critical need to develop nanoprobes capable of sensing biotargets and molecular signaling processes within single living cells, thus providing the important information for biomedical research and clinical applications. Fiber-optic nanosensors are suitable for sensing intracellular/intercellular physiological and biological parameters in submicron environments. Optical fibers having nanoscale tips were developed initially to serve as scanning probes in near-field optical microscopes (NSOM) (*1*). The development of one such probe capable of obtaining measurements with a spatial sub-wavelength resolution was then reported (*2*). Due to its high spatial resolution (sub-wavelength), near-field microscopy has received great interest and has been used in many applications (*3, 4*). Over the last two decades our laboratory has been interested in the investigation and development of fiberoptic chemical sensors and biosensors for environmental and biochemical monitoring (*5-11*). The combination of NSOM and Raman spectroscopy was used to achieve sub-wavelength 100-nm spatial resolution (*12, 13*). Single-molecule detection and imaging schemes using nanofibers could open new capabilities in the investigation of the complex biochemical reactions and pathways in biological systems at the single cell level leading to important applications in medicine and health effect studies.

A. Development of Optical Nanoprobes for Single-cell Monitoring

*A.1 Design and Fabrication of Fiber-optic Nanoprobes*

Fiber-optic nanoprobes can be fabricated with the laser pulling method, which consists of local heating of an optical fiber using a laser and subsequently pulling the fiber apart. Fabrication of nanosensors requires techniques capable of making reproducible optical fibers with submicron-size diameter core. As the laser pulling process is a time-dependent heating effect, a variety of factors like laser power, timing of pulling, velocity setting and pulling force are all contribute to the taper shape and tip size. Since transmission efficiency is highly dependent on the taper shape, it is crucial to control the tip shape in the fabrication of high-quality nanoprobes. Figure 1 illustrates the experimental procedures for the fabrication of nanofibers using the micropipette puller (Sutter Instruments P-2000). A scanning election microscopy (SEM) photograph of one of the fiber probes fabricated for studies is shown in Figure 2. The distal end of the nanofiber is approximately 40 nm (*14, 15*).

The sidewall of the tapered end is then coated with a thin layer of metal, such as silver, aluminum or gold to prevent light leakage of the excitation light on the tapered side of the fiber. Such a coating system is illustrated in Figure 3. An array of fiber probes is attached on a rotating motor inside a thermal evaporation chamber. While the probes are rotated, the metal is allowed to evaporate onto the tapered side of the fiber tip to form a thin coating. The fiber is pointing away from the evaporation source with an angle of approximately 25°. The tapered end was coated with ~75-100 nm of metal in a thermal evaporator (Quorum Technologies E6700). With the metal coating, the size of the probe tip is approximately 200-250 nm. Due to the inclination angle, the tip ends are shadowed from evaporation when the fiber tips are tilted away from the source. A nano-aperture was formed on the tip end for optical excitation and subsequent binding with bioreceptors. The size of the nanoaperture is related to the angle between fiber axis and evaporation direction. It was found that nanoaperture diameters of approximately 50 nm can be achieved using a 25° tilt angle (Figure 4B). However, if the angle is less than 20°, most of the fibers are fully covered with metal and no aperture is visible using SEM (Figure 4A). On the contrary, if the angle is higher than 30°, a larger area of the distal end of the fiber tip will be exposed (Figure 4C). It is

critical to control the inclination angle to obtain fiber-optic nanoprobes. The inclination angle is affected by the fiber taper angle and the setup in the coating system.

The metallic coating process is a critical step in nanoprobe fabrication. A thin film of an opaque metal such as aluminum, silver or gold is coated along the outside walls of the tapered optical fiber tip to form an optical light pipe free of defects, which would permit photons to escape from the tapered sides of the optical fiber. An optical aperture to allow evanescent wave excitation is formed at the tip's apex by angled evaporation. Gold has higher melting temperature (660°C for Al, 960°C for Ag and 1060°C for Au) and better thermal resistance. The thermal stress generated during metallic film deposition damages the aperture due to very different thermal expansion coefficients of metal and quartz. Gold coating has the lowest thermal expansion coefficient ($23.1\times10^{-6}$ /°C for Al, $18.9\times10^{-6}$ /°C for Ag, $14.2\times10^{-6}$ /°C for Au, $0.55\times10^{-6}$ /°C for $SiO_2$) which will reduce the thermal destruction of the fiber tip. Further, gold coatings are more stable in ambient conditions. Silver coating gives the strongest enhancement in surface-enhanced Raman scattering (SERS) nanoprobe, which has been applied in our plasmonic nanobiosensing (*16*). However, silver is susceptible to attack by oxygen and constituents of atmospheric pollution, such as chlorine, sulfur and ozone. When these substances react with the silver layer, it becomes tarnished so that the required optical properties are lost. Aluminum is a desirable material to use in NSOM-type optical nanoprobe because it has the highest extinction coefficient of all metals. Aluminum also adheres to fibers more firmly than silver or gold so that no adhesion layer is required and general cleaning does not affect the coating. However, it is difficult to evaporate aluminum as a thin film while maintaining smooth films with small grain sizes. The grainy feature not only causes light leaking but also blocks the nanoaperture. The grain diameter is highly and sensitively dependent on the deposition pressure. Below $5\times10^{-6}$ torr, the size of the individual grains is smaller than 100 nm. There was a relationship between rate of metallic deposition and subsequent surface roughness, and studies revealed that a slower coating rate (<5 Å/s) resulted in better smoothness and the film opacity required for our intended sensor applications.

Fiber-optic nanoprobe with nanoscale aperture at the tapered end of the fiber involves carefully coating a metal layer without blocking the optical throughput. The nanoaperture only forms under optimized tilt angle during shadow evaporation of metal coating onto the fiber tip (*14, 15, 17*). It is critical to fabricate probes with well-controlled nanoapertures for optimal spatial resolution and optical transmission. Traditional manufacturing processes still limit the quality of metal coated fiber probes. Optical throughput of pulled nanoprobes is limited by the sharp taper angle. Another method of fabrication nanoprobes involves chemical etching. Chemical etched tips have higher throughput; however, they do not have a flat distal end as the laser pulled ones which are difficult to form well-defined nano-apertures in shadow evaporation. Moreover, shadow evaporation often leads to either complete or irregular coated tips. Grainy structures of metal thin film increase the distance between the aperture and the sample which reduce the resolution and intensity. It is easy to form pin holes at the taper region that causes leaking. The aperture also deviates from ideal circular shape because of grains. A quantitative analysis of probe transmission efficiency becomes difficult.

The detection sensitivity of fiber optic nanoprobe depends mainly on the extremely small excitation volume which is determined by the aperture sizes and penetration depths. The size of nanoaperture is difficult to control as the metal grains can easily block the aperture. Using focused ion beam (FIB) milling, we have demonstrated that optical nanoprobes with well-defined aperture size as small as 200 nm can be fabricated (Figure 5). In order to fabricate well defined fiber-optic nanoprobe tips, we employed focused ion beam (FIB) milling of nanoapertures in the metallic films deposited on tapered tips of optical fibers. Before carrying out FIB milling, the optical fibers were coated with metallic films (aluminum, silver or gold) using electron beam evaporation (CHA Industries Solution E-Beam) or thermal evaporation. During the evaporation process, the fiber-optic tips faced the metal source to ensure that the fiber side walls and the tips were completely covered with a thin metallic layer (100-150 nm). The sample mount was rotated to improve uniformity and the thickness of the metallic film was monitored by a quartz crystal monitor. The deposition rate was varied between 0.05 nm $s^{-1}$ and 0.2 nm $s^{-1}$ at a chamber pressure of ~$3\times10^{-6}$ Torr for the electron beam evaporated films. A Hitachi FB2100 Focused Ion Beam milling machine with a gallium ion source was used to fabricate the nanoapertures on the fiber tips. Beam currents and accelerating voltages of 0.01 nA and 40 keV energy were typically used. The desired nanostructures were milled by rastering the ion beam and employing a beam blanker. The beam blanker shuts on and off according to a 8-bit grayscale, 512 by 512 pixel image file. Tapered optical fiber tips with nanoapertures were fabricated by

employing FIB milling at magnifications varying between 3000x and 18000x depending on the desired minimum aperture size. To form metallic nanostructures on the tips of optical fibers, a special fiber holder that could fit in the FIB stage was fabricated. The angle of evaporation is not necessary in FIB, therefore reducing the chance of pin-hole formation. Milling of the nanoapertures using this process has an advantage that it is not time consuming as several tips placed adjacent to each other can be cut with the same beam raster, it gives reliable nanoprobes with well-defined nanoapertures of circular geometry, and the length of the optical fiber nanoprobes can be longer which can make coupling of light into the optical fibers easier. A clean aperture free from grains also facilitates the subsequent functionalization of bioreceptor molecules on the fiber distal end for biosensing applications. FIB processing is a promising technique in nanoprobe fabrication in addition to laser pulling and chemical etching.

*A.2 Characterization of Fiber-optic Nanoprobe by NSOM*

The optimal angle of inclination can be determined through characterization of nanoapertures under SEM. The SEM can determine the actual size of the tip aperture. However, having a nanometer-sized aperture does not guarantee a good near-field probe. The tip aperture, even though it may appear small on the SEM, could be a result of over-coating, and hence not be a functional light aperture at all. Therefore, a functional scan is necessary to reveal the near-field effect from the probe. NSOM enables functional analysis of the nanosensor probe by performing an NSOM scan on a standard sample, e.g. a Fischer pattern (Figure 6A). The standard sample usually consists of patterns with size less than the diffraction limits ($0.5\lambda$) that can be determined by an atomic force microscope. The nanosensor probe was attached to an NSOM system working as an NSOM probe. Typically, the aperture of the probe roughly determines the resolution of the image. In other word, the image quality thus represents the quality of the probe. The figures show that a good-quality probe yields an NSOM image that resolves clearly the hexagonal pattern (Figure 6B) while a slightly broken probe results in a blurry image (Figure 6C). For subsequent nanosensor detection, only the good quality probes were used.

*A.3 Theoretical Modeling of the Probing Depth of a Typical Optical Nanoprobe*

We analytically characterized the exponentially decaying near-field laser excitation through the subwavelength aperture. The power calculation was performed in two steps. First, the mode matching theory was used to investigate the relationship between the transmitted power out of a nano-sized aperture in front of a tapered fiber and the fiber's parameters. Figure 7A shows the transmitted power relative to the incident power as a function of the half cone angle for various aperture sizes. It is evident from Figure 7A that the transmitted power increases with bigger aperture size; furthermore, the larger the cone angle is, the greater the transmitted power. Therefore it is desirable to use a fiber with a large cone angle to maximize the transmitted power. The second step was to estimate the near-field light distribution in the vicinity of the fiber aperture using the Bethe-Bouwkamp's solution (as in an infinite metal screen). Figure 7B shows the averaged electric field intensity as a function of the distance from the aperture for various aperture sizes. The laser wavelength was 325 nm. Figure 7C shows the distribution of averaged electric field intensity on a plane that passes through the central axis of the fiber. It can be seen that the field intensity drops more quickly when the aperture size becomes smaller. For example, the probing depth of a nanoprobe with a 50-nm aperture using a HeCd laser (325 nm) will reach ~200 nm, hence all the molecules in that 200 nm region beyond the aperture (Figure 7C) should be sufficiently excited upon laser illumination to be detected by the fluorescence measurements.

*A.4 Functionalization of Fiber-optic Nanoprobe*

We have investigated several approaches for antibody immobilization. These include physical absorption, layer-by-layer (LBL) assembly, and covalent attachment, and eventually chose the covalent attachment as the optimal method. The tapered end of the optical fiber was first activated for antibody immobilization. Specifically, a probe, which was determined to be of good quality by an NSOM functional scan of a standard sample, was submerged in 3-Aminopropyltriethoxysilane (APTS) (1% pH 5.5) solution for 1 h. Afterward the probe was rinsed with water and cured at 110 ºC for 30 min. The amine-surface can be modified to contain carboxylate groups involving the reaction with glutaric anhydride (saturation in DMF) for 2 h. The probe was rinsed with DMF and then with water. To active the carboxyl groups to NHS esters for coupling with amine-containing biomolecules, the probe was immersed in N-hydroxysuccinimide (NHS) (1 M) and N,N9-dicyclohexylcarbodiimide (DCC) (1 M)

solution for 2 h and rinse with DMF. The activated fiber was incubated for 3 h, at room temperature, in monoclonal antibody (Mab) (0.05 mg/ml in PBS) and rinsed with PBS several times. Nonspecific binding sites on the optical fiber were blocked afterwards, by treating the tapered end with PBS/Bovine serum albumin (BSA) (~2 mg/ml) for 2 h. The fiber was stored in PBS at 4°C.

C. Investigation of Fiber-optic Nanoprobe in Single Living Cell

*C.1 Fiber-optic Nanoprobe for Detection of Chemical Species in Single Living Cell*

Prior to developing nanobiosensors for testing real-time signaling in live breast cancer cells, it is important to evaluate the nanosensors to monitor fluorescent compounds in single cells. Chemical analysis of polynuclear aromatic hydrocarbons (PAHs) is of great environmental and toxicological interest because many of them have been shown to be mutagens and/or potent carcinogens in laboratory animal assays. Benzo[a]pyrene (BaP), which has been extensively investigated, is one of the more potent carcinogens among PAHs and is a fundamental indicator of exposure and carcinogenic activity of all PAHs. In order to facilitate the study of intracellular dynamics of benzo[a]pyrene tetrol (BPT), the related biomarker under BaP exposure, a quantitative estimation of the numbers BPT molecules detected using fiber optic nanoprobes for solutions containing different BPT concentrations was performed. Our results demonstrated the feasibility of antibody-functionalized nanobiosensors for the sensitive detection of a biologically significant species (e.g. benzo[a]pyrene tetrol or BPT) used as the model system in single cells (*17*).

The optical measurement system used for nanoprobe is schematically illustrated in Figure 8. For nanoprobe measurements, the 325 nm line of a HeCd laser (CVI Melles Griot, 15 mW laser power) was focused onto a 400 μm delivery fiber. A tapered fiber was coupled to the delivery fiber through a capillary tubing and was secured to the micromanipulators (Narishige MLW-3) on a Zeiss Axiovert 200M microscope (Zeiss). The fluorescence emitted from the region beyond the aperture was collected by the microscope objective and passed through a bandpass filter (386 nm) and then focused onto a photomultiplier tube (PMT, Hamamatsu, HC125-2) for detection. The output from the PMT was recorded on a universal counter (Agilent 53131A), and a personal computer (PC) was used for further data treatment. Nanoprobes were also used to investigate BPT in single cells. PC3 human prostate cancer cells were incubated with 1 μM BPT in PBS for 2 h. Control cells are treated with PBS only. All dishes were rinsed with PBS prior to measurement. Nanoprobes were controlled by the micromanipulator to puncture the cell and keep inside while taking the measurement. Figure 9 shows the intracellular measurement of BPT in PC3 human prostate cancer cells. The cells were incubated with $1e^{-6}$ M BPT in PBS for 2 h. Control cells are treated with PBS only. All dishes were rinsed with PBS prior to measurement. It was apparent that treated cells had higher fluorescence readings than thise in the control group. The limit of detection was determined to be less than 100 molecules for BPT from the calibration curve (*17*). Although in our preliminary experiments the living cells were directly incubated with BPT, the results illustrate that the nanoprobes can be employed to detect very low concentrations of fluorescent species such as BPT molecules that are important biomarkers of exposure and carcinogenic activity of related PAHs, inside living cells. We expect the above configuration can be applied for protein phosphorylation measurement by immobilizing corresponding antibodies on the nanoprobe and choosing the right light sources and filters with respect to the fluorophores.

*C.2 Investigation of Fiber-optic Nanoprobe in Breast Cancer Cells*

We have developed SERS-active fiber-optic nanoprobes for real-time intracellular biosensing (*16, 18*). Fiber-optic nanoprobes circumvent all concerns regarding inhomogeneous dye diffusion, slow rates of nanoparticle uptake, and difficulty defining intracellular nanoparticle trajectories. In addition, because the SERS substrate is physically anchored to the nanoprobes as a statistically-random silver island film (AgIF), we can avoid concerns regarding the dynamic nanoparticle aggregation effects which typically prevent use of SERS for quantitative intracellular bioanalysis. We have used SERS-active fiber-optic nanoprobes to measure the intracellular pH of HMEC-15/hTERT immortalized human mammary epithelial cells, PC-3 human prostate cancer cells, MCF-7 human breast cancer cells and breast cancer cells acquired from the Duke High-Risk Cohort via Random Periareolar Fine Needle Aspiration (RPFNA) (*16, 18*). Briefly, the SERS-based nanoprobes are produced by tapering 400-μm diameter optical fibers using a pipette puller, yielding fiber tips which are typically

~50 nm in diameter (Figure 10a, inset). The tapered optical fibers are then coated with a 6-nm mass thickness of silver, producing a film of nanoscopic silver islands (e.g. a "silver island film" or "AgIF") which enhances the Raman scattering intensity of nearby molecules. In our proof-of-concept studies, the nanoprobes were made pH-sensitive across the physiological range via silver-thiol attachment of para-mercaptobenzoic acid (pMBA). The SERS spectrum of pMBA between 1350 and 1450 $cm^{-1}$ changes with pH (Figures 10b and 10c). Below pH 6, the SERS intensity in this region is weak and the band profile is broad. Deprotonation above pH 6 increases the SERS intensity (Figure 10c) and shifts the peak maximum from ~1405 $cm^{-1}$ to ~1425 $cm^{-1}$. The location and intensity of this SERS band relative to the ~1587 $cm^{-1}$ combination band are established indicators of intracellular pH (*19*). After functionalization with pMBA, we use micromanipulators to insert these SERS-active, pH-sensitive nanoprobes into cells adhered to fibronectin-coated fused silica microscope slides or embedded in Matrigel™. The time required for insertion and interrogation is typically < 1 minute and, as with in vitro fertilization, the cells generally show no visible signs of stress (e.g. blebbing, detachment from the microscope slide, decrease in pH, etc.). Figure 10d shows SERS spectra from a pH-sensitive nanoprobe inside (blue) and outside (red) a MCF-7 human BC cell in pH 7.4 phosphate buffered saline (PBS). The spectra are essentially identical, except for the pH-sensitive region between 1350 and 1450 cm-1. The intracellular pH of the cell shown in Figure 10a is 6.8 ± 0.1 based on the calibration curve in Figure 10c. This agrees with the known average pH of MCF-7 cells (*20*). The extracellular pH is 7.3 ±0.1, matching the pH of the PBS.

Following up on our initial studies, we have most recently applied our pH-sensitive SERS-based nanoprobes to intracellular pH determination of breast cells acquired from the Duke High-Risk Cohort via RPFNA, a research procedure developed to test for the presence of a "high-risk field" in women at risk for breast cancer and to monitor cellular response to prevention (*21, 22*). Figure 11a shows a white-light image of a SERS-based, pH-sensitive nanoprobe inserted in one of these patient cells, and highlights the ease with which fiber-optic nanoprobes can be used to selectively interrogate cells of interest in a complex matrix (e.g., a mixture of Matrigel™ and RPFNA aspirate containing lipid, red blood cells, etc.). Figure 11b shows single spectra collected for 10 sec from a nanoprobe in MatrigelTM (top trace), using the same nanoprobe inside the patient cell shown in Figure 11a (middle trace) and the same cell in the absence of the nanoprobe (bottom trace). Unlike the cultured cells used in our initial proof-of-concept work, the complex RPFNA aspirate matrix can have a strong, well-defined Raman signature (Figure 11b, bottom trace) characterized by Raman scatter from nucleic acids, proteins, lipids, etc. The spectrum of the nanoprobe within the cell (Figure 11b, middle trace) is a convolution of this intrinsic background and the pH-sensitive SERS spectrum of pMBA (Figure 11b, top trace). Simple one-to-one subtraction of the intrinsic Raman background associated with the patient cells from the combined cell + FON spectrum yields a recognizable (albeit noisy) pMBA spectrum (Figure 11c). The SNR can be further improved by extending the acquisition time from 10 seconds to a few minutes or, alternatively, by improving the SERS enhancement of the nanoprobes.

Our results to date have been promising in that we have consistently detected intracellular pH values similar to the expected pH of ~7.2 – 7.3. This data confirms that nanoprobe insertion and interrogation in patient cells, as in cultured cells, (A) produces no significant lysosomal response or (B) can be performed rapidly enough that highly-acidic lysosomes are unable to seek out and attack the SERS-based nanoprobes. In either case, the potential to use more biochemically- and biomedically-relevant sensing chemistries is clear. In addition, we have demonstrated that insertion and interrogation of the pH-sensitive, SERS-active nanoprobe induces neither apoptosis nor an aggressive lysosomal response from either of these cell lines. These results demonstrate the robustness of the SERS-active pH nanoprobe for intracellular pH measurements and point toward the potential utility of additional biochemically specific fiber-optic nanoprobes.

*C3. Multiplex Detection of Breast Cancer Biomarker Using Plasmonic Nanoprobes*

The ability to simultaneously detect multiple oligonucleotide sequences is critical for many medical applications such as early diagnosis, high-throughput screening and systems biology research. In particular, the development of practical and sensitive detection techniques with multiplexing capability can lead to improved accuracy for cancer diagnosis, since a variety of molecular alterations in multiple genes are usually involved in tumorigenesis and progression of various cancers. Nanoparticle-based SERS nanoprobes have great potential for multiplexed

DNA detection for medical diagnostics and high-throughput bioassays. These nanoprobes can be attached to nanofiber tips for biosensing.

We have demonstrated the feasibility of multiplex detection using the SERS-based molecular sentinel (MS) technology in a homogeneous solution (*23*). Figure 12 schematically illustrates the operating principle of the MS nanoprobe. The MS nanoprobe is composed of a DNA hairpin probe (~30–45 nucleotides (nt) in length) and a metal (e.g., silver) nanoparticle. One end of the hairpin probe is tagged with a SERS-active label as a signal reporter. At the other end, the probe is modified with a thiol group, which is designed to conjugate covalently to the silver nanoparticle via thiol–metal interaction. The sequence within the loop region of the hairpin probe is complementary to a specific target gene sequence of interest. In the absence of the target, the Raman label is in close proximity to the metal surface due to the stem-loop configuration ('closed' state), and a strong SERS signal is produced upon laser excitation. The metal nanoparticle is used as a signal enhancing platform for the SERS signal associated with the label. The enhancement is due to a nanostructured metal surface scattering process (nano-enhancers) which increases the intrinsically weak normal Raman scattering. The enhancement mechanism for SERS comes from intense localized fields arising from surface plasmon resonance in metallic (e.g. Ag, Au, Cu) nanostructures with sizes in the order of tens of nanometers and from chemical effects at the metal surface (*24*).

Two MS nanoprobes tagged with different Raman labels were used to detect the presence of the *erbB-2* and *ki-67* breast cancer biomarkers. The multiplexing capability of the MS technique was demonstrated by mixing the two MS nanoprobes and tested in the presence of single or multiple DNA targets. To further demonstrate the specificity and selectivity of the composite MS nanoprobes, the hybridization assays were then performed in the presence of individual complementary DNA target (i.e. only one of the two complementary targets). The middle and lower spectra in Figure 13 show the resulted SERS signal from the composite MS nanoprobes targeted to 0.5 μM target DNA complementary to ERBB2-MS and KI67-MS nanoprobes, respectively. The result indicates that only the SERS peaks associated with the complementary MS nanoprobes was significantly quenched (indicated by arrows) when in the presence of its target DNA.

The results of this study demonstrate the specificity and selectivity of the MS nanoprobes, as well as the ability to use multiple MS nanoprobes for multiplexed DNA detection. Furthermore, the SERS measurements were performed immediately following the hybridization reactions using a homogeneous assay without washing steps, which greatly simplifies the assay procedures. The results of this study demonstrate that the MS nanoprobe technique can provide a useful tool for multiplexed DNA detection in a homogeneous solution for medical diagnostics and high-throughput bioassays. The MS nanoprobe technology can be integrated with nanofibers for biosensing applications in breast cancer monitoring and diagnostics.

**KEY RESEARCH ACCOMPLISHMENTS:**

- Optimized fabrication of optical nanoprobe by angled evaporation and FIB milling to improve spatial resolution and optical transmission
- Characterized fiber-optic nanoprobes with SEM and NSOM to insure best performance
- Determined the probing depth and volume of the nanoprobe through theoretical modeling
- Demonstrated fiber-optic nanoprobes in the sensitive detection of biologically significant species in single living cells
- Demonstrated SERS-active fiber optic nanoprobe for intracellular pH measurement in human breast cancer cells
- Demonstrated multiplex detection of breast cancer biomarker using plasmonic nanoprobes

**REPORTABLE OUTCOMES:**

**Journal paper**

1. T. Vo-Dinh, Y. Zhang, Single-cell monitoring using fiberoptic nanosensors. *Wiley Interdiscip Rev Nanomed Nanobiotechnol* **3**, 79 (Jan-Feb, 2011).
2. Y. Zhang, A. Dhawan, T. Vo-Dinh, Design and Fabrication of Fiber-Optic Nanoprobes for Optical Sensing. *Nanoscale Res Lett* **6**, (2011).
3. J. P. Scaffidi, M. K. Gregas, B. Lauly, S. DeVience, V. Seewaldt, T. Vo-Dinh, Minimally invasive intracellular pH measurement in cultured and patient-derived cells using plasmonic fiber-optic nanoprobes. (Manuscript to be submitted).

**Patent application**

1. T. Vo-Dinh, H. Wang, Nanonetwork plasmonics coupling interface and methods of use. 61/497,315 (2011).

**CONCLUSION:**

Fiber-optic nanoprobes provide important tools for minimal invasive analysis at single cellular or sub-cellular level. In this study, we have optimized fabrication of fiber-optic nanoprobes through angled evaporation and FIB milling. Because transmission efficiency is highly related to the aperture size, control of the nanoaperture size is essential in the fabrication of high-quality nanoprobes. Subtle changes in the tilt angle during metal evaporation can greatly affect the size or even the existence of the aperture. A much more rational fabrication process would involve a nanofabrication technique such as FIB, in which aperture size could be independently controlled from evaporation. Metallic coating process is an essential step to prevent photons to escape from the tapered side of the optical fiber. Coating conditions such as air pressure and coating rate need to be carefully controlled to form metal layers with less defects. Nanoprobes can be characterized with SEM and NSOM to reveal their performance. Theoretical modeling is useful to optimize the shape and size of the nanoprobe. Our research has led to successful designing and fabrication of fiber-optic nanoprobes having optimized performance. We have demonstrated the fiber-optic nanoprobes in the sensitive detection of biologically significant species in single living cells and intracellular pH measurement in human breast cancer cells from the Duke High-Risk Cohort via RPFNA. Monitoring single cells with fiber-optic nanoprobes have opened up new applications in molecular biology and medical diagnostics in breast cancer. Nanoparticle-based SERS nanoprobes have great potential for multiplexed DNA detection for medical diagnostics and high-throughput bioassays. These nanotools can be used to study intracellular signaling processes and to investigate gene expression inside single living cells. Probing sub-cellular architecture and dynamic processes is essential in understanding the fundamental biological processes such as cell signaling pathways in a systems biology approach. Single-cell monitoring is also important in studies where the amount of cells obtained is limited, which could not be analyzed with other techniques. Future development of this nanosensor technology will lead to multi-analyte detection and high-throughput screening at the single-cell level.

**REFERENCES:**


1. D. W. Pohl, in *Advances in Optical and Electron Microscopy,* C. J. R. Sheppard, T. Mulevy, Eds. (Academic, London, 1991), vol. 12, pp. 243-312.
2. E. Betzig, R. J. Chichester, Single Molecules Observed by near-Field Scanning Optical Microscopy. *Science* **262**, 1422 (Nov 26, 1993).
3. A. Hartschuh, Tip-enhanced near-field optical microscopy. *Angew Chem Int Ed Engl* **47**, 8178 (2008).
4. R. X. Bian, R. C. Dunn, X. S. Xie, P. T. Leung, Single molecule emission characteristics in near-field microscopy. *Phys Rev Lett* **75**, 4772 (Dec 25, 1995).
5. J. P. Alarie, J. R. Bowyer, M. J. Sepaniak, A. M. Hoyt, T. Vodinh, Fluorescence Monitoring of a Benzo[a]Pyrene Metabolite Using a Regenerable Immunochemical-Based Fiberoptic Sensor. *Analytica Chimica Acta* **236**, 237 (Sep 17, 1990).
6. J. P. Alarie, T. Vodinh, A Fiberoptic Cyclodextrin-Based Sensor. *Talanta* **38**, 529 (May, 1991).
7. B. M. Cullum, G. D. Griffin, G. H. Miller, T. Vo-Dinh, Intracellular measurements in mammary carcinoma cells using fiber-optic nanosensors. *Analytical Biochemistry* **277**, 25 (Jan 1, 2000).
8. B. M. Cullum, T. Vo-Dinh, The development of optical nanosensors for biological measurements. *Trends in Biotechnology* **18**, 388 (Sep, 2000).
9. P. M. Kasili, J. M. Song, T. Vo-Dinh, Optical sensor for the detection of caspase-9 activity in a single cell. *Journal of the American Chemical Society* **126**, 2799 (Mar 10, 2004).
10. T. Vo-Dinh, Nanosensing at the single cell level. *Spectrochimica Acta Part B-Atomic Spectroscopy* **63**, 95 (Feb, 2008).
11. T. Vo-Dinh, J. P. Alarie, B. M. Cullum, G. D. Griffin, Antibody-based nanoprobe for measurement of a fluorescent analyte in a single cell. *Nature Biotechnology* **18**, 764 (Jul, 2000).
12. V. Deckert, D. Zeisel, R. Zenobi, T. Vo-Dinh, Near-field surface enhanced Raman imaging of dye-labeled DNA with 100-nm resolution. *Analytical Chemistry* **70**, 2646 (Jul 1, 1998).
13. D. Zeisel, V. Deckert, R. Zenobi, T. Vo-Dinh, Near-field surface-enhanced Raman spectroscopy of dye molecules adsorbed on silver island films. *Chemical Physics Letters* **283**, 381 (Feb 13, 1998).
14. T. Vo-Dinh, Y. Zhang, in *Handbook of Nanophysics: Nanomedicine and Nanorobotics*. (CRC Press, 2010).
15. T. Vo-Dinh, Y. Zhang, Single-cell monitoring using fiberoptic nanosensors. *Wiley Interdiscip Rev Nanomed Nanobiotechnol* **3**, 79 (Jan-Feb, 2011).
16. J. P. Scaffidi, M. K. Gregas, V. Seewaldt, T. Vo-Dinh, SERS-based plasmonic nanobiosensing in single living cells. *Analytical and Bioanalytical Chemistry* **393**, 1135 (Feb, 2009).
17. Y. Zhang, A. Dhawan, T. Vo-Dinh, Design and Fabrication of Fiber-Optic Nanoprobes for Optical Sensing. *Nanoscale Res Lett* **6**, (2011).
18. J. P. Scaffidi *et al.* (Manuscript to be submitted).
19. J. Kneipp, H. Kneipp, B. Wittig, K. Kneipp, One- and two-photon excited optical ph probing for cells using surface-enhanced Raman and hyper-Raman nanosensors. *Nano Letters* **7**, 2819 (Sep, 2007).
20. M. Schindler, S. Grabski, E. Hoff, S. M. Simon, Defective pH regulation of acidic compartments in human breast cancer cells (MCF-7) is normalized in adriamycin-resistant cells (MCF-7adr). *Biochemistry* **35**, 2811 (Mar 5, 1996).
21. G. R. Bean *et al.*, Morphologically normal-appearing mammary epithelial cells obtained from high-risk women exhibit methylation silencing of INK4a/ARF. *Clin Cancer Res* **13**, 6834 (Nov 15, 2007).
22. J. C. Baker, Jr. *et al.*, ESR1 promoter hypermethylation does not predict atypia in RPFNA nor persistent atypia after 12 months tamoxifen chemoprevention. *Cancer Epidemiol Biomarkers Prev* **17**, 1884 (Aug, 2008).
23. H. N. Wang, T. Vo-Dinh, Multiplex detection of breast cancer biomarkers using plasmonic molecular sentinel nanoprobes. *Nanotechnology* **20**, 065101 (Feb 11, 2009).
24. A. Campion, P. Kambhampati, Surface-enhanced Raman scattering. *Chemical Society Reviews* **27**, 241 (Jul, 1998).

**SUPPORTING DATA:**

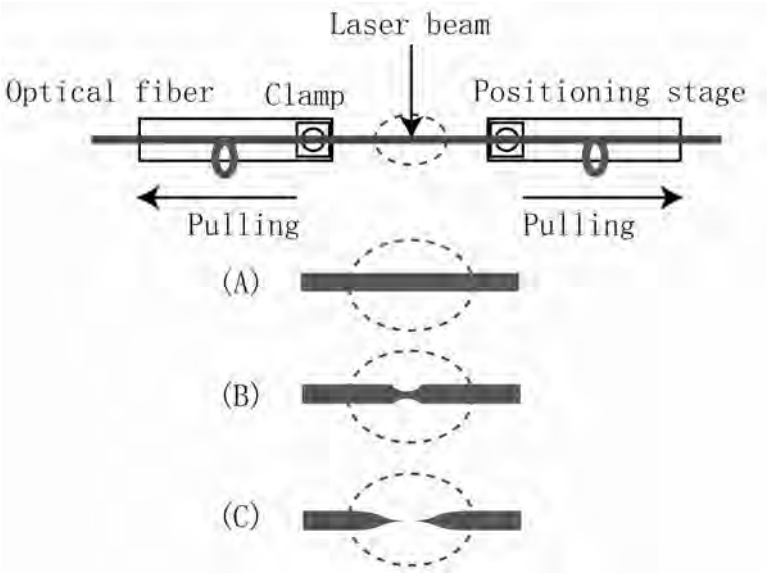


**Figure1**. The fabrication of nanofibers through laser pulling. (A)-(C) represent the course of pull in time. In (C) a nanotip has been formed.

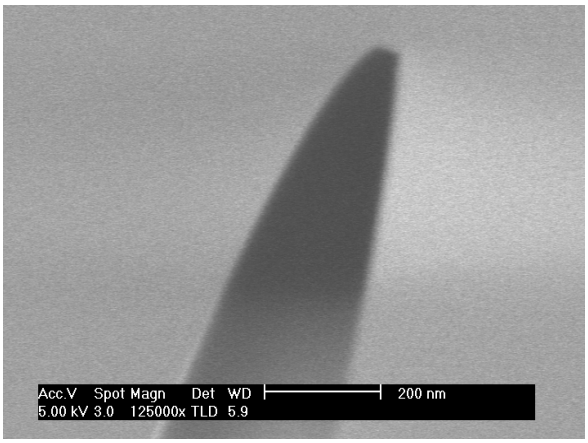


**Figure 2**. Scanning electron photograph of an uncoated nanofiber

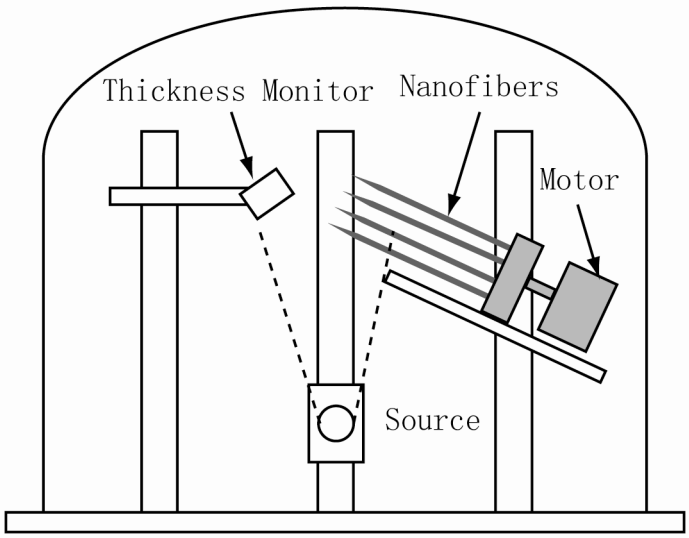


**Figure 3**. Angle evaporation of nanofibers in a thermal evaporator.

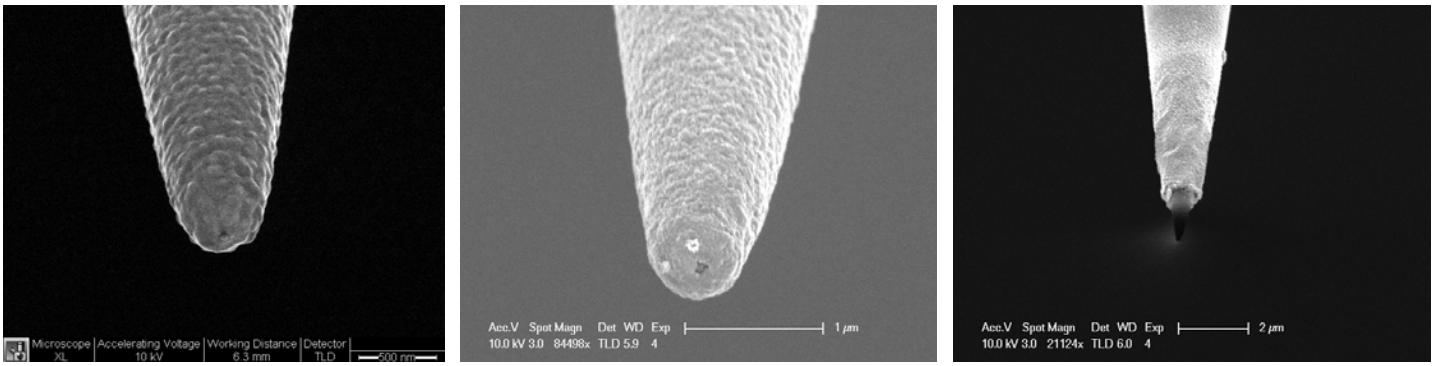


**A** **B** **C**

**Figure 4**. Nanofibers coated with silver at different inclination angles A) 20° B) 25° C) 30°.

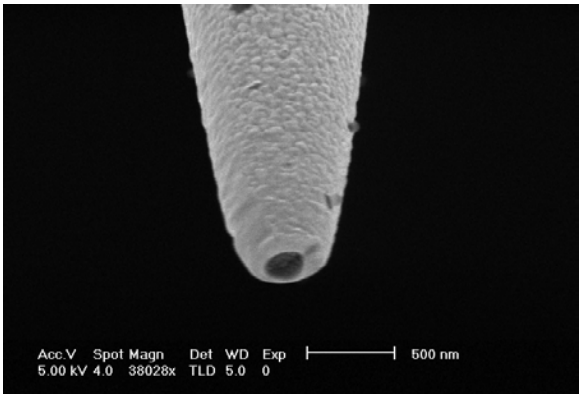


**Figure 5**. FIB-etched nanoprobe with aperture diameter of 200 nm.

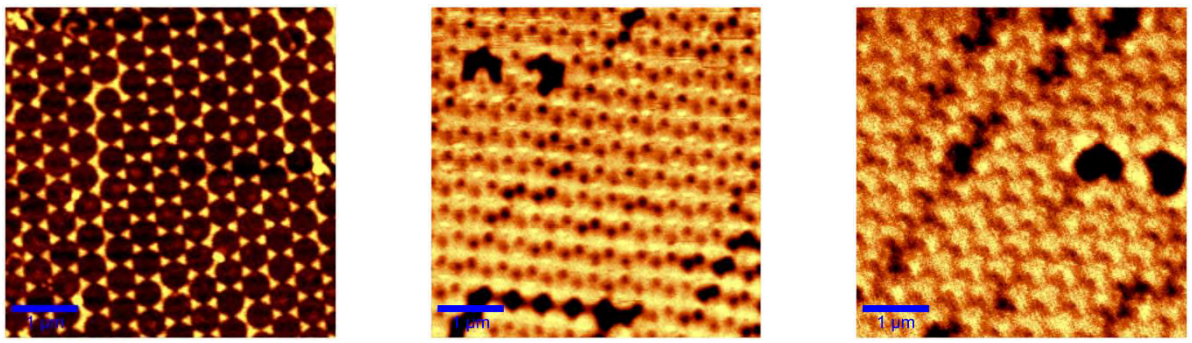


A B C

**Figure 6**. A) An AFM image (2x2um) of a Fischer pattern of 453nm pitch and 150nm-sided triangles, and NSOM images (5 µm × 5µm) of a Fischer pattern using Witec alpha300s with a standard 100nm-aperture probe (in a transmission mode) from B) a good tip, and C) a broken tip.

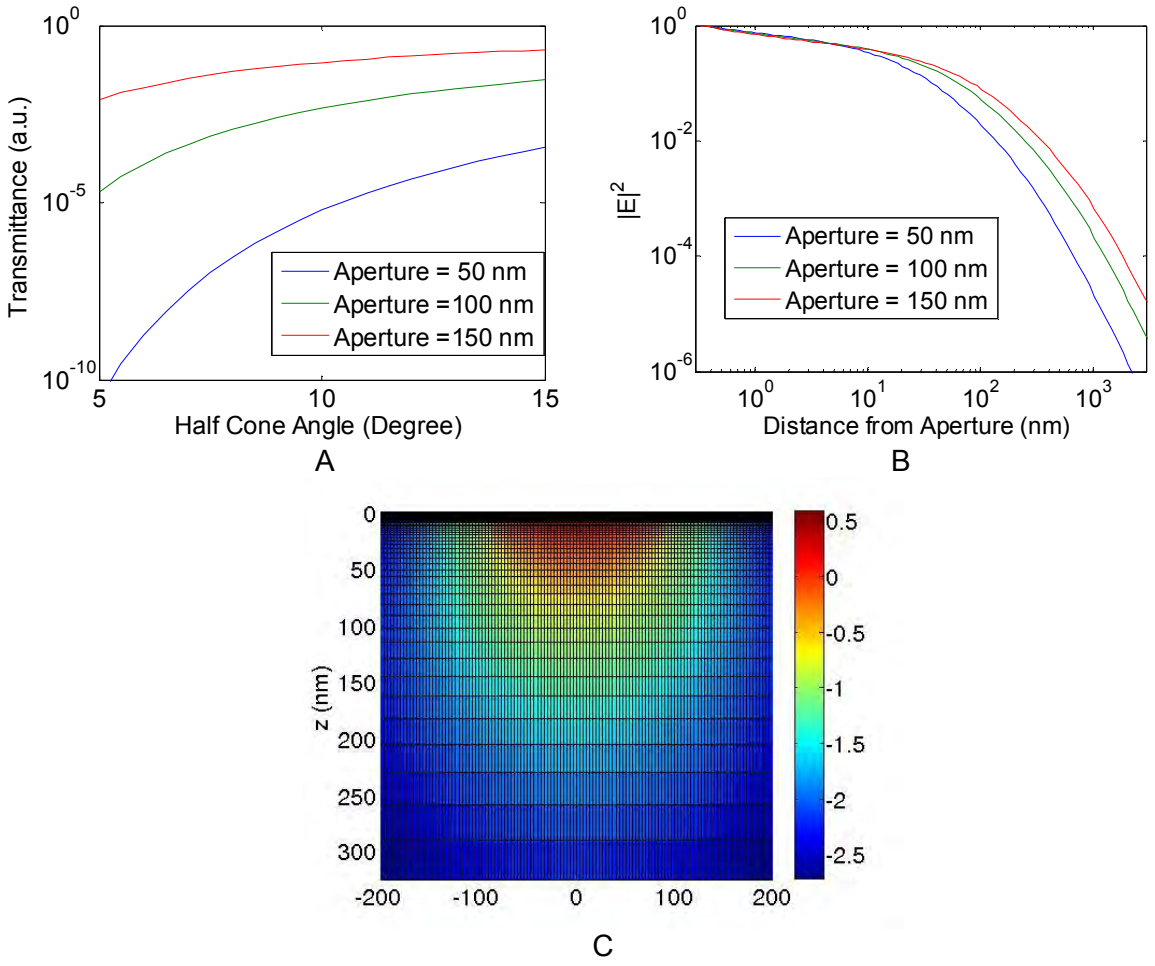


A B C

**Figure 7**. A) Output power as a function of the half cone angle for various aperture sizes of a tapered fiber, B) The averaged electric field intensity as a function of the distance from the aperture for various aperture sizes calculated by Bethe-Bouwkamp's solution, and C) Distribution of averaged electric field intensity across the plane y = 0. The horizontal axis is x-axis. The intensity has been processed by log10 function to enhance contrast. The laser wavelength used for simulation: 325 nm.

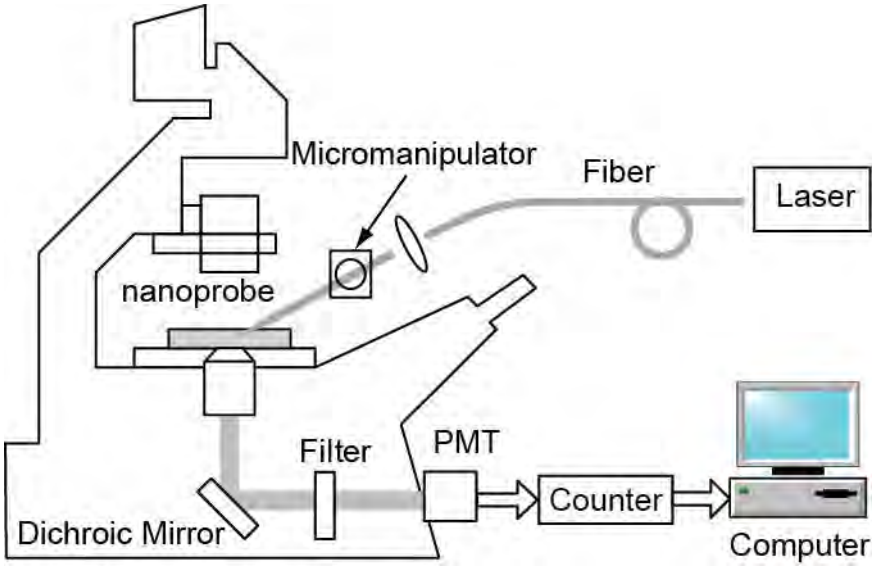


**Figure 8**. Instrumental system for fluorescence measurements using nanoprobes.

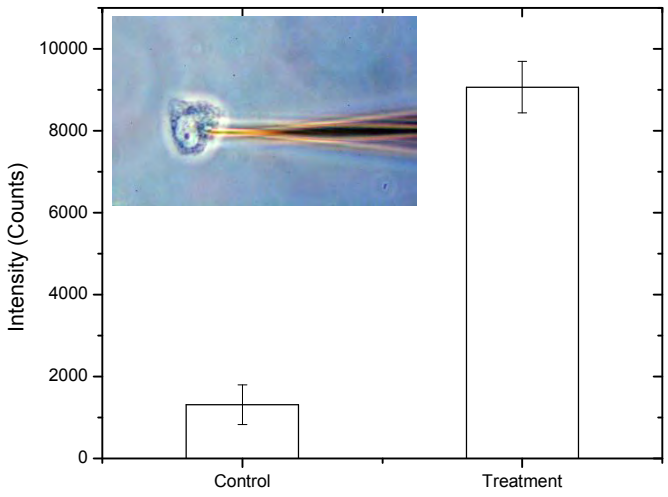


**Figure 9.** Intracellular measurement of Benzopyrene tetrol with nanosensor. PC3 human prostate cancer cells were incubated with 1e-6M BPT in PBS for 2 h. Control cells are treated with PBS only. All dishes were rinsed with PBS prior to measurement. Insert picture is a nanosensor inside a human cancer cell.

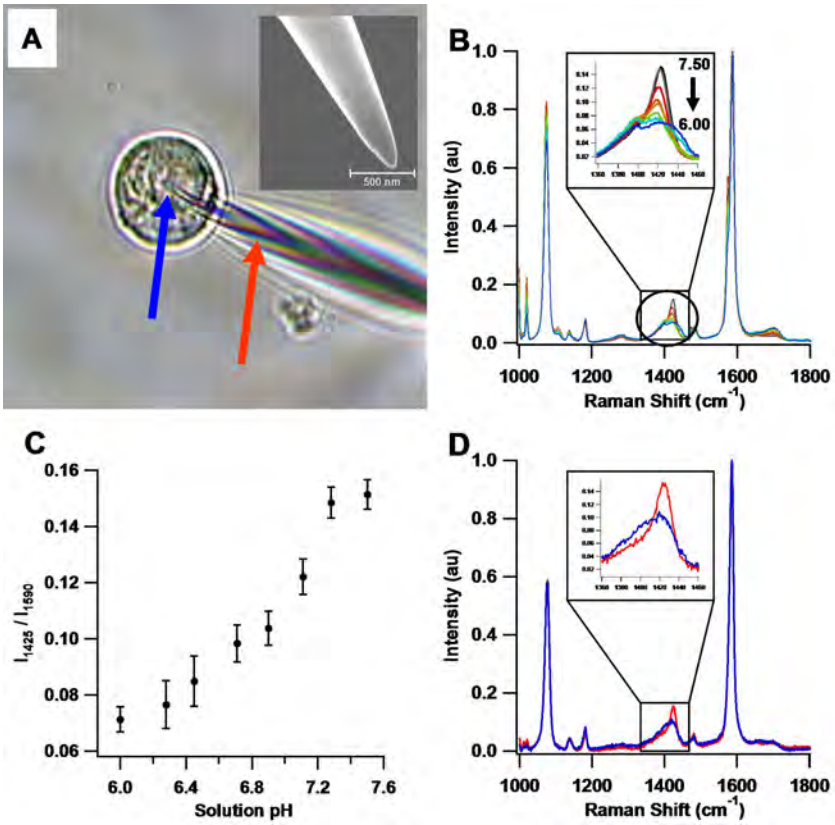


**Figure 10**. Intracellular pH sensing in single living cultured cells using SERS-based fiber-optic nanoprobes (FON). (A) image of a pH-sensitive, SERS-active FON interrogating a MCF-7 breast cancer cell; (B) illustration of the pH dependence of the SERS spectrum from the pH-sensitive FONs; (C) pH calibration curve acquired from ten individual pH-sensitive FONs; (D) single ten-second SERS spectra acquired from points inside (blue) and outside (red) the cell shown in (A). The buffer pH is 7.4, and the intracellular pH is ~6.8.

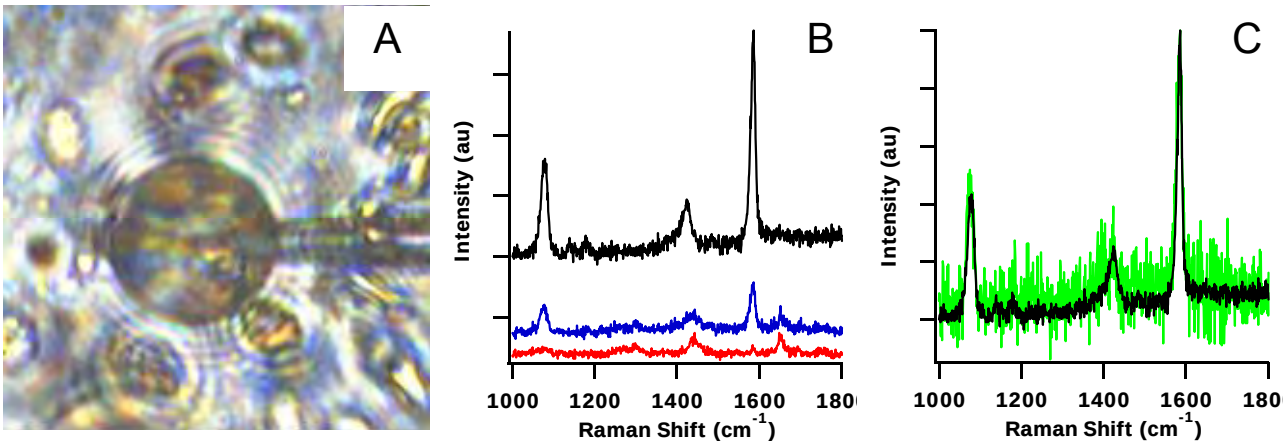


**Figure 11**. Intracellular pH sensing with patient cells acquired via RPFNA. (A) White-light image of a pH-sensitive fiber-optic nanoprobe (FON) interrogating a patient cell embedded in Matrigel™. (B) Top: SERS spectrum of a FON in Matrigel™ at pH ~7.3; Middle: Spectrum of the same FON in the patient cell shown in (A); Bottom: Intrinsic Raman spectrum of the patient cell in (A). (C) Green: Unsmoothed, untreated difference spectrum produced by direct one-to-one subtraction of the cell's intrinsic Raman spectrum (B, bottom) from the FON + cell spectrum (B, middle). Black: SERS spectrum of the pH-sensitive FON at pH 7.3 (B, top), included to guide the eye.

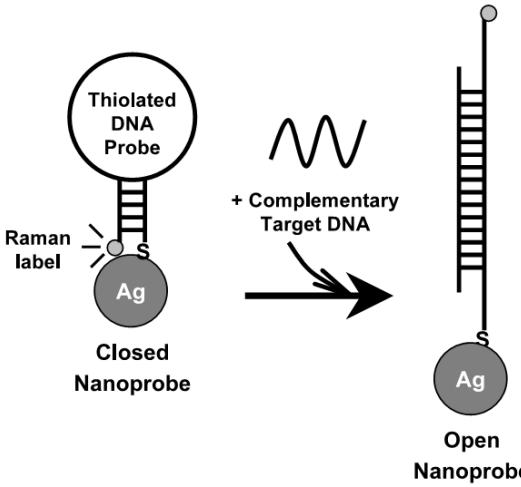


**Figure 12**. The operating principle of the SERS-based molecular sentinel (MS) nanoprobes. The MS nanoprobe is composed of a Raman-labeled DNA hairpin probe and a silver nanoparticle. In the absence of the complementary target DNA, a strong SERS signal is observed due to the hairpin conformation adopted by the MS nanoprobe (left: closed state). In the presence of the complementary target DNA, the hairpin conformation of the MS nanoprobe is disrupted and the SERS signal is quenched due to the physical separation of the Raman label from the surface of the silver nanoparticle (right: open state).

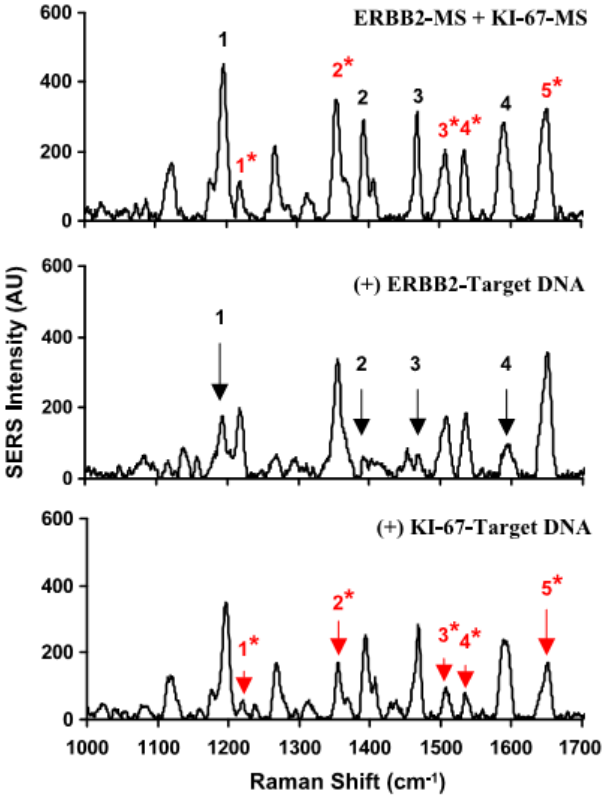


**Figure 13**. SERS spectra of the composite MS nanoprobes (ERBB2-MS + KI-67-MS) in the presence or absence of single target DNA. The major Raman bands from ERBB2-MS are marked with black number, and the major Raman bands from KI-67-MS are marked with red number with (*) sign. Upper spectrum: blank (in the absence of any target DNA). Middle spectrum: in the presence of single target DNA complementary to the ERBB2-MS nanoprobes. Lower spectrum: in the presence of single target DNA complementary to the KI-67-MS nanoprobes. The arrow signs illustrate the decreased SERS intensity of the major Raman bands in the presence of corresponding target DNA.

**APPENDICES:**

Please see attached papers.

Nanoscale Research Letters
a SpringerOpen Journal

NANO EXPRESS Open Access

# Design and Fabrication of Fiber-Optic Nanoprobes for Optical Sensing

Yan Zhang[1,2], Anuj Dhawan[1,2], Tuan Vo-Dinh[1,2,3*]

**Abstract**

This paper describes the design and fabrication of fiber-optic nanoprobes developed for optical detection in single living cells. It is critical to fabricate probes with well-controlled nanoapertures for optimized spatial resolution and optical transmission. The detection sensitivity of fiber-optic nanoprobe depends mainly on the extremely small excitation volume that is determined by the aperture sizes and penetration depths. We investigate the angle dependence of the aperture in shadow evaporation of the metal coating onto the tip wall. It was found that nanoaperture diameters of approximately 50 nm can be achieved using a 25° tilt angle. On the other hand, the aperture size is sensitive to the subtle change of the metal evaporation angle and could be blocked by irregular metal grains. Through focused ion beam (FIB) milling, optical nanoprobes with well-defined aperture size as small as 200 nm can be obtained. Finally, we illustrate the use of the nanoprobes by detecting a fluorescent species, benzo[a] pyrene tetrol (BPT), in single living cells. A quantitative estimation of the numbers of BPT molecules detected using fiber-optic nanoprobes for BPT solutions shows that the limit of detection was approximately 100 molecules.

## Introduction

The emergence of nanotechnology opens new horizons for nanosensors and nanoprobes that are suitable for intracellular measurements. Nanosensors provide critical information for monitoring biomolecular processes within a single living cell, thus could provide great advances in biomedical research and clinical applications. Fiber-optic nanosensors with nanoscale dimensions are capable of sensing intracellular/intercellular physiological and biological parameters in submicron environments. Tapered fibers with distal diameters between 20 and 500 nm have been demonstrated for near-field scanning optical microscopy (NSOM) [1,2]. Chemical nanosensors were developed for monitoring calcium and nitric oxide, among other physico-chemicals in single cells [3,4]. Vo-Dinh and coworkers have developed nanobiosensors to detect biochemical targets inside living single cells [5-12]. Fiber-optic nanoprobe promises to be an area of growing research that could potentially provide an imaging tool for monitoring individual cells and even biological molecules. Single-molecule detection and imaging schemes using nanofibers could open new possibilities in the investigation of the complex biochemical reactions and pathways in biological and cellular systems leading to important applications in medicine and health effect studies.

Optical nanotips were first developed as scanning probes in near-field optical microscopes [2]. Such nanoprobes can achieve resolution as high as λ/50, where λ is the wavelength of light [1]. It is important to control aperture size, taper shape, and metal coating to achieve a better performance [13]. The fiber-optic probes were fabricated by laser-heated pulling or chemical etching [14-16]. Laser-pulled fiber tips can achieve diameters smaller than 50 nm with small cone angles [14]. Chemical etching tips have larger cone angles and similar apex sizes [15]. However, it is often difficult to control the etching process. The side of the fiber was further coated with silver, aluminum, or gold films to confine the light [9,14,17]. Traditional manufacturing processes still limit the quality of metal-coated fiber probes. Optical throughput of pulled nanoprobes is limited by the sharp taper angle. Chemical-etched tips have higher throughput; however, they do not have a flat distal end as laser-pulled ones which are difficult to form well-defined nanoapertures in shadow evaporation. Moreover, shadow evaporation often leads to either complete or irregular coated tip. Grainy structures of metal thin film increase

* Correspondence: tuan.vodinh@duke.edu
[1]Fitzpatrick Institute for Photonics, Duke University, Durham, NC 27708, USA. Full list of author information is available at the end of the article

the distance between the aperture and the sample, which reduce the resolution and intensity. It is also easy to form pin holes at the tapered region that could cause light-leaking. The aperture deviates from ideal circular shape because of grains. A quantitative analysis of probe transmission efficiency becomes difficult. Focused ion beam (FIB) fabrication of nanostructures has been applied on optical fibers for chemical sensing [18]. FIB milling for nanostructure formation allows precise control of size and shape in nanometer accuracy. This paper deals specifically with the metal coating on the formation of nanoaperture at the tip end. Coating materials and angles greatly affect the quality of the nanoprobe. By combining with focused ion beam milling, nanoprobes with well-defined aperture as small as 200 nm have been obtained. We investigate the capacity of the nanoprobes by detect benzo[a]pyrene tetrol in living cells.

## Experimental Procedures

### Nanoprobe Fabrication

Optical nanoprobes were fabricated through laser pulling method, which consists of local heating of an optical fiber (Polymicro Technologies FVP400440480) using a laser and subsequently pulling the fiber apart. Fabrication of nanosensors requires techniques capable of making reproducible optical fibers with submicron-size-diameter core. Figure 1 illustrates the experimental setup for the fabrication of nanofibers using the micropipette puller (Sutter Instruments P-2000) [9]. As the laser pulling process is a time-dependent heating effect, laser power, timing of pulling, velocity setting, and pulling force all contribute to the taper shape and tip size. Since transmission efficiency is highly dependent on the taper shape, it is crucial to control the tip shape in the fabrication of high-quality nanoprobes.

The sidewall of the tapered end was then coated with a thin layer of metal, such as silver, aluminum, or gold to prevent light leakage of the excitation light on the tapered side of the fiber. An array of fiber probes was attached on a rotating motor inside a thermal evaporation chamber (Quorum Technologies E6700). The rotation rate was controlled by a microcontroller board (Parallax). While the probes were rotating, the metal was allowed to evaporate onto the tapered side of the fiber tip to form a thin coating. The nanoaperture was formed through shadowed evaporation as the fibers were tilting away from the source. The nanoprobes were characterized with scanning electron microscopy (FEI XL30).

In order to fabricate well-defined fiber-optic nanoprobe tips, we employed focused ion beam (FIB) milling of nanoapertures in the metallic films deposited on tapered tips of optical fibers. Before carrying out FIB milling, the optical fibers were coated with metallic films (aluminum, silver or gold) using electron beam evaporation (CHA Industries Solution E-Beam). During the evaporation process, the fiber-optic tips faced the metal source to ensure that the fiber side walls and the tips were completely covered with a thin metallic layer (100–150 nm). The sample mount was rotated to improve uniformity and the thickness of the metallic film was monitored by a quartz crystal monitor. The deposition rate was varied between 0.05 and 0.2 nm $s^{-1}$ at a chamber pressure of ~3 × $10^{-6}$ Torr for the electron beam evaporated films.

A Hitachi FB2100 focused ion beam milling machine with a gallium ion source was used to fabricate the nanoapertures on the fiber tips. Beam currents and accelerating voltages of 0.01 nA and 40 keV energy were typically used. The desired nanostructures were milled by rastering the ion beam and employing a beam blanker. The beam blanker shuts on and off according to a 8-bit grayscale, 512 by 512 pixel image file. Tapered optical fiber tips with nanoapertures were fabricated by employing FIB milling at magnifications varying between 3000× and 18000× depending on the desired minimum aperture size. To form metallic nanostructures on the tips of optical fibers, a special fiber holder that could fit in the FIB stage was fabricated.

### Optical Measurement

The optical measurement system used for nanoprobe is schematically illustrated in Figure 2. For nanoprobe measurements, the 325 nm line of a HeCd laser

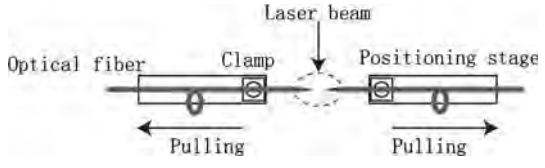


**Figure 1 Fabrication of nanofibers by laser pulling.**

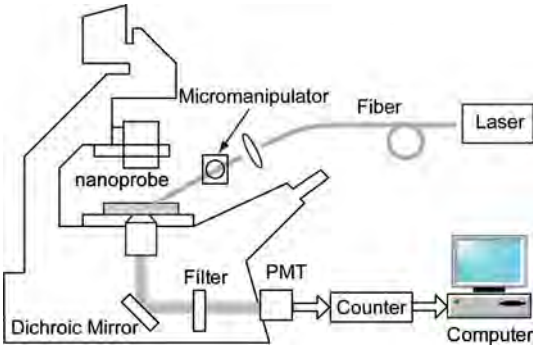


**Figure 2 Instrumental system for fluorescence measurements using nanoprobes.**

(CVI Melles Griot, 15 mW laser power) was focused onto a 400 μm delivery fiber. A tapered fiber was coupled to the delivery fiber through a capillary tubing and was secured to the micromanipulators (Narishige MLW-3) on a Zeiss Axiovert 200M microscope (Zeiss). The fluorescence emitted from the region beyond the aperture was collected by the microscope objective and passed through a bandpass filter (386 nm) and then focused onto a photomultiplier tube (PMT, Hamamatsu, HC125-2) for detection. The output from the PMT was recorded on a universal counter (Agilent 53131A), and a personal computer (PC) was used for further data treatment.

Nanoprobes were also used to investigate BPT in single cells. PC3 human prostate cancer cells were incubated with 1 μM BPT in PBS for 2 h. Control cells are treated with PBS only. All dishes were rinsed with PBS prior to measurement. Nanoprobes were controlled by the micromanipulator to puncture the cell and keep inside while taking the measurement.

## Results and Discussion

### Effect of the Metal Evaporation Angle

A scanning election microscopy (SEM) photograph of one of the nanofibers fabricated by the laser pulling method is shown in Figure 3a. The distal end of the nanofiber is approximately 40 nm. The fiber was pointing away from the evaporation source with an angle of approximately 25°. The tapered end was coated with ~75–100 nm of metal in the thermal evaporator. With the metal coating, the size of the probe tip is approximately 200–250 nm (Figure 3b).

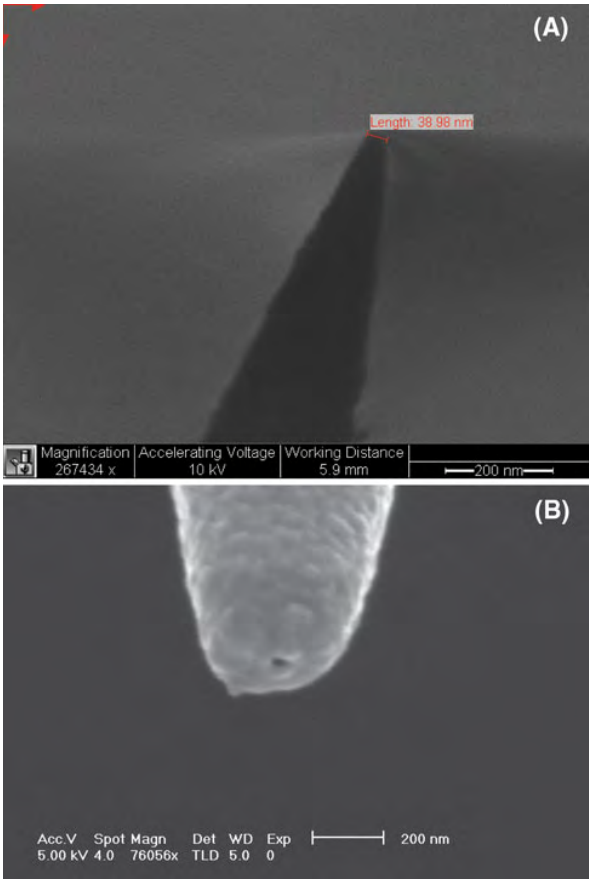


**Figure 3 SEM images of a an uncoated nanofiber and b a gold-coated nanofiber**.

Due to the inclination angle, the tip ends are shadowed from evaporation when the fiber tips are tilted away from the source. The effect of shadow evaporation angle is illustrated in Figure 4. A nanoaperture was formed on the tip end for optical excitation. The size of the nanoaperture is related to the angle between fiber axis and evaporation direction. For example, if the angle is less than 20°, most of the fibers are fully covered with metal and no aperture is visible using SEM. On the contrary, if the angle is higher than 30°, a larger area of the distal end of the fiber tip will be exposed (Figure 5). The optimal angle of inclination can be determined through characterization of nanoapertures under SEM. The SEM can determine the actual size of the tip aperture. However, having a nanometer-sized aperture does not guarantee a good near-field probe. The tip aperture, even though it may appear small on the SEM, could be a result of aluminum over-coating, and hence not be a functional light aperture for actual measurements. Therefore, a functional scan is necessary to reveal the near-field effect from the probe. Near-field scanning optical microscope (NSOM) enables functional analysis of the nanosensor probe by performing a scan on a standard sample, e.g., a Fischer pattern. The standard sample usually consists of patterns with size less than the diffraction limits (0.5 λ) that can be determined by an atomic force microscope. The nanosensor probe was attached to an NSOM system working as an NSOM probe. Typically, the aperture of the probe roughly determines the resolution of the image. In other word, the image quality thus represents the quality of the probe.

### Effect of the Different Metal Coatings on the Nanoprobes

The metallic coating process is a critical step in nanoprobe fabrication. A thin film of an optically opaque metal such as aluminum, silver, or gold is coated along the outside walls of the tapered optical fiber tip to form an optical light pipe free of defects, which would permit photons to escape from the tapered sides of the optical fiber. An optical aperture to allow evanescent wave excitation is formed at the tip's apex by angled evaporation. Silver has been used in nanoprobe fabrication [9]. It has high reflectivity in the visible and IR range and very stable in aqueous solutions as long as oxidizing agents

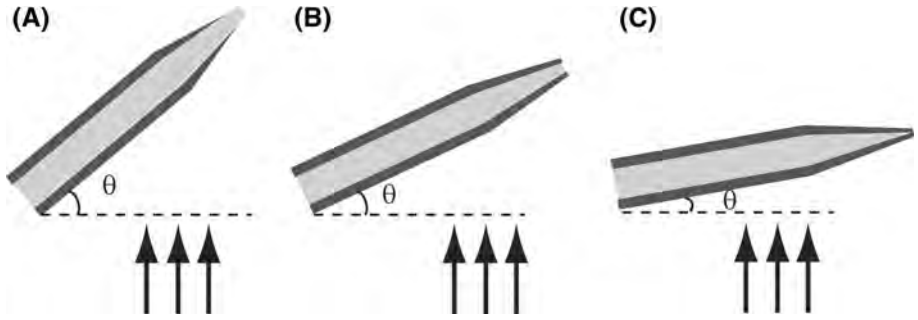


**Figure 4 Nanoaperture formation by shadow evaporation with a high angle (>25°), b medium angle (~25°), and c low angle (<25°).**

or complexing agents are not present. But a silver layer will oxidize rapidly under ordinary atmospheric conditions and will not exhibit a high reflectance below 400 nm. Therefore, it is desirable to use the nanoprobe right after metal evaporation. Otherwise, the light shielding will deteriorate or even the coating will peel off after a few days in air.

Gold thin film was demonstrated to be a very stable coating under environmental conditions although it does not have high reflectance in visible range. An interface layer such as Cr is required to increase adhesion between gold and the fiber silica surface. Gold has a high melting temperature (660°C for Al, 960°C for Ag, and 1,060°C for Au) and a good thermal resistance. The thermal stress generated during metallic film deposition damages the aperture due to very different thermal expansion coefficients of metal and quartz. Gold coating has the lowest thermal expansion coefficient ($23.1 \times 10^{-6}$/°C for Al, $18.9 \times 10^{-6}$/°C for Ag, $14.2 \times 10^{-6}$/°C for Au, $0.55 \times 10^{-6}$/°C for $SiO_2$), which will reduce the thermal destruction of the fiber tip.

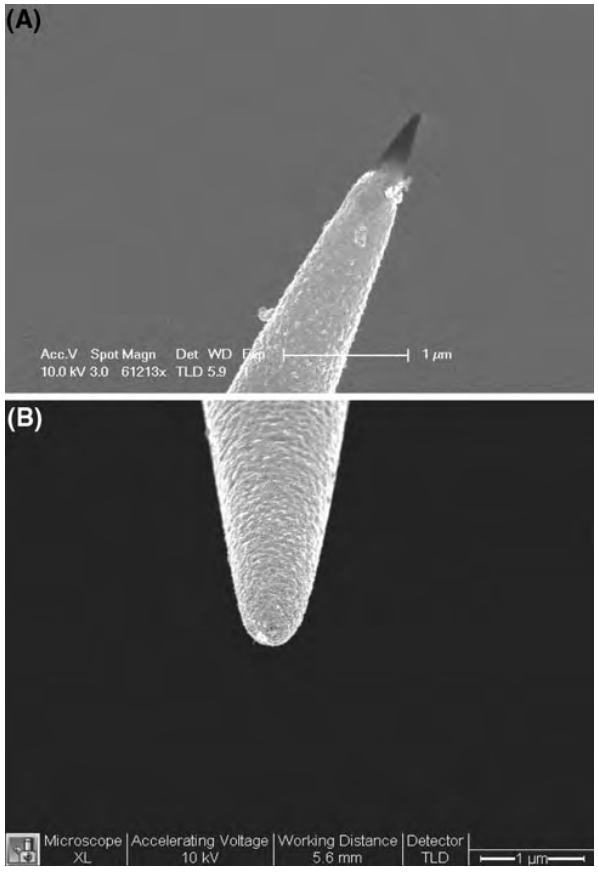


**Figure 5 SEM images of silver-coated nanofibers under different angles: a 40° and b 20°.**

Aluminum is a desirable material to use because it has the highest extinction coefficient of all metals. Aluminum adheres to fibers more firmly than silver or gold so that no interface layer is required and general cleaning does not affect the coating. Figure 6 compares the nanofibers after argon plasma cleaning (Emitech K-1050X, 100 W, 5 min). Silver coatings are easily peeled off while aluminum coatings exhibit no changes under the same condition. Aluminum is inert toward corrosive agents since a protective oxide layer is formed readily upon contact to the air. However, it is difficult to evaporate aluminum as a thin film while maintaining smooth films with small grain sizes [19]. Grainy films contribute to the high background in near-field sensing. The grain diameter is highly and sensitively dependent on the deposition pressure. Below $5 \times 10^{-6}$ torr, the size of the individual grains is smaller than 100 nm. There was a relationship between rate of metallic deposition and subsequent surface roughness, and studies revealed that higher coating rate (>10 nm/s) resulted in better smoothness and the film opacity required for our intended sensor applications.

### Nanoprobe Fabrication using Focus Ion Beam (FIB) Milling

The first FIB milling process involved placing the metal-coated optical fiber tips horizontally, i.e., orthogonal to the focused ion beam and then cutting the tips (both the tapered silica fiber and the metal over-coating) such

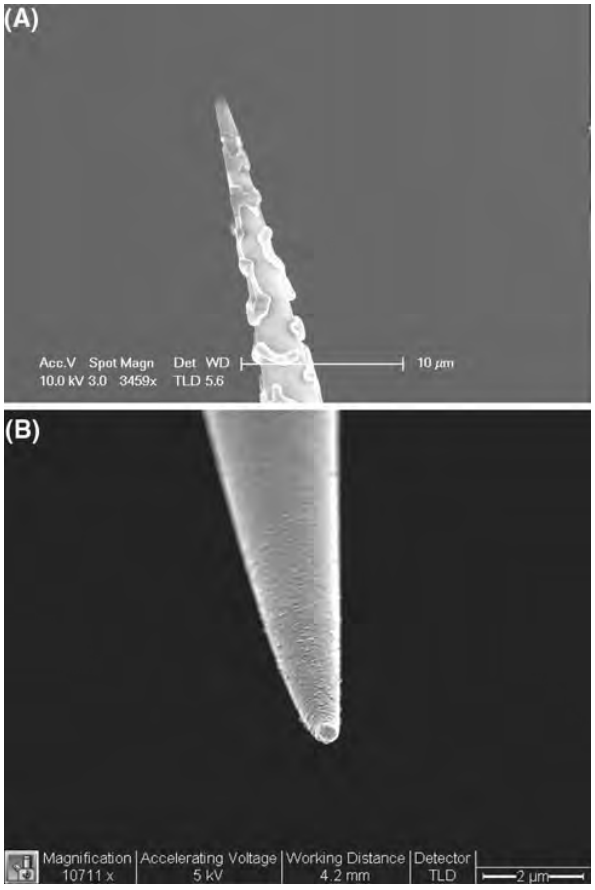


**Figure 6 SEM images of a silver- and b aluminum-coated nanofibers after plasma cleaning**.

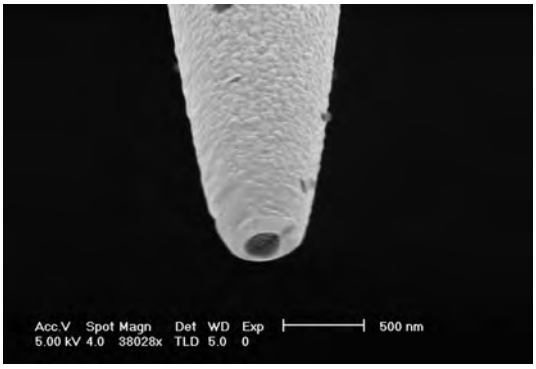


**Figure 7 FIB-etched nanoprobe with aperture diameter of 200 nm**.

that an aperture could be developed at the tip. Milling of the nanoapertures using this process has an advantage that it is not time-consuming as several tips placed adjacent to each other can be cut with the same beam raster, it gives reliable nanoprobes with well-defined nanoapertures of circular geometry, and the length of the optical fiber nanoprobes can be longer, which can make coupling of light into the optical fibers easier. The second process involved positioning the fiber tips such that they faced the focused ion beam and then carrying out the milling of the nanoapertures at the tip. Although this process enables fabrication of nanoapertures of different geometries and sizes in a very controllable manner, it limits the length of the fiber-optic probe as only a certain length of the optical fiber probe can be placed vertically in the Hitachi FB2100 focused ion beam milling machine. By milling with a focused ion beam, an aperture with controllable shape and diameter as small as 200 nm was achieved (Figure 7). The angle of evaporation is not necessary in FIB, therefore reducing the chance of pin-hole formation. A clean aperture free from grains also facilitates the subsequent functionalization of bioreceptor molecules on the fiber distal end for biosensing applications. FIB processing is a promising technique in nanoprobe fabrication in addition to laser pulling and chemical etching.

### Fluorescence Measurement of Benzo[a]Pyrene Tetrol (BPT) Using Nanoprobes

Chemical analysis of polynuclear aromatic hydrocarbons (PAHs) is of great environmental and toxicological interest because many of them have been shown to be mutagens and/or potent carcinogens in laboratory animal assays. Benzo[a]pyrene (BaP), which has been extensively investigated, is one of the more potent carcinogens among PAHs and is a fundamental indicator of exposure and carcinogenic activity of all PAHs. In order to facilitate the study of intracellular dynamics of benzo [a]pyrene tetrol (BPT), the related biomarker under BaP exposure, a quantitative estimation of the numbers BPT molecules detected using fiber-optic nanoprobes for solutions containing different BPT concentrations was performed and shown in Figure 8. The limit of detection that corresponds to the amount of analyte emitting a signal 3 times the standard deviation of the noise was determined to be 1 μM for BPT. Under 1 μM, the dark count noise from PMT was stronger than the signal. The detection volume can be estimated as 17 aL for 200 nm aperture probe based on Bethe–Bouwkamp theory. Therefore, the limit of detection was approximately 100 BPT molecules. Figure 9 shows the intracellular measurement of BPT in PC3 human prostate cancer cells. The cells were incubated with 1 μM BPT in PBS for 2 h at 37°C. Control cells are PC3 cells treated with PBS only. All dishes were rinsed with PBS prior to measurement. It is apparent that the treated cells exhibited higher fluorescence reading than the control group. Although in our preliminary experiments the living cells were directly incubated with BPT, the results illustrate

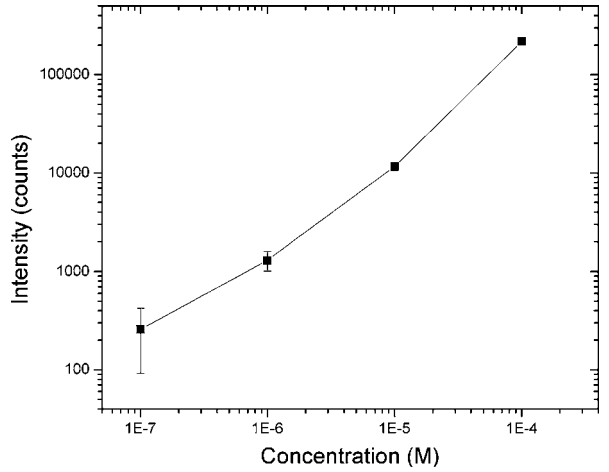


**Figure 8 Fluorescence intensities of benzo[a]pyrene tetrol (BPT) measured with a fiber-optic nanoprobe**.

that the nanoprobes can be employed to detect very low concentrations of fluorescent species such as BPT molecules that are important biomarkers of exposure and carcinogenic activity of related PAHs, inside living cells.

## Conclusion

Fiber-optic nanoprobes have opened up new applications in molecular biology and medical diagnostics. Due to their small sizes, nanosensor provides important tools for minimal invasive analysis at single cellular or subcellular level. Because transmission efficiency is highly related to the aperture size, control the nanoaperture size is essential in the fabrication of high-quality nanoprobes. Subtle changes in the tilt angle during metal evaporation can greatly affect the size or even the existence of the aperture. A much more rational fabrication process would involve a nanofabrication technique such as FIB, in which aperture size could be independently controlled from evaporation. The detection sensitivity of fiber-optic nanoprobes depends mainly on the extremely small excitation or detection volume set by the aperture sizes and penetration depths. This effectively reduces background fluorescence, thereby enhance detection sensitivity. Nanofabrication would also greatly improve the reproducibility of aperture shapes and hence the optical performance of near-field probes.

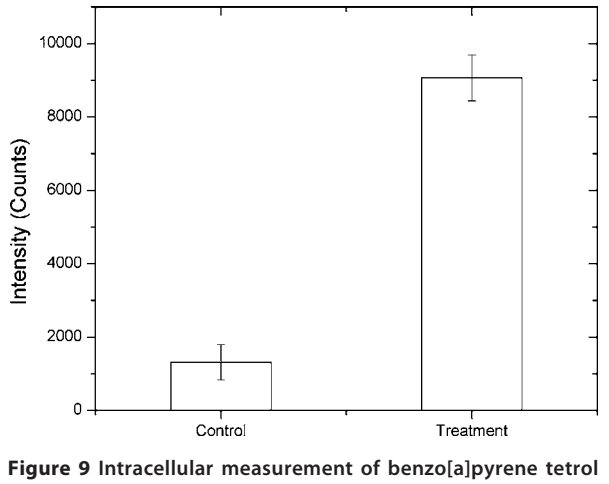


**Figure 9 Intracellular measurement of benzo[a]pyrene tetrol (BPT) with nanoprobes**. PC3 human prostate cancer cells were incubated with 1 μM BPT in PBS for 2 h. Control cells are treated with PBS only. All *dishes* were rinsed with PBS prior to measurement.

**Acknowledgements**

The author acknowledges the contribution of G.D. Griffin, J.P. Alarie, B.M. Cullum, and P. Kasili. This research is sponsored by the National Institutes of Health (1R01ES014774 and R01-EB006201) and US Army Medical Research and Material Command (W81XWH-09-1-0064).

**Author details**

[1]Fitzpatrick Institute for Photonics, Duke University, Durham, NC 27708, USA. [2]Department of Biomedical Engineering, Duke University, Durham, NC 27708, USA. [3]Department of Chemistry, Duke University, Durham, NC 27708, USA.

Received: 7 July 2010 Accepted: 5 August 2010
Published: 31 August 2010

**References**

1. Betzig E, Chichester RJ: *Science* 1993, **262**:1422-1425.
2. Pohl DW: **Advances in Optical and Electron Microscopy.** Academic London; 1991:**12**:243-312.
3. Tan WH, Shi ZY, Kopelman R: *Anal Chem* 1992, **64**:2985-2990.
4. Tan WH, Shi ZY, Smith S, Birnbaum D, Kopelman R: *Science* 1992, **258**:778-781.
5. Cullum BM, Griffin GD, Miller GH, Vo-Dinh T: *Anal Biochem* 2000, **277**:25-32.
6. Kasili PM, Song JM, Vo-Dinh T, Am J: *Chem Soc* 2004, **126**:2799-2806.
7. Song JM, Kasili PM, Griffin GD, Vo-Dinh T: *Anal Chem* 2004, **76**:2591-2594.
8. Vo-Dinh T: *Spectrochim Acta, Part B* 2008, **63**:95-103.
9. Vo-Dinh T, Alarie JP, Cullum BM, Griffin GD: *Nat Biotechnol* 2000, **18**:764-767.
10. Vo-Dinh T, Griffin GD, Alarie JP, Cullum BM, Sumpter B, Noid DJ: *J Nanopart Res* 2000, **2**:17-27.
11. Vo-Dinh T, Kasili P: *Anal Bioanal Chem* 2005, **382**:918-925.
12. Vo-Dinh T, Kasili P, Wabuyele M: *Nanomedicine* 2006, **2**:22-30.
13. Essaidi N, Chen Y, Kottler V, Cambril E, Mayeux C, Ronarch N, Vieu C: *Appl Opt* 1998, **37**:609-615.
14. Valaskovic GA, Holton M, Morrison GH: *Appl Opt* 1995, **34**:1215-1228.
15. Stockle R, Fokas C, Deckert V, Zenobi R, Sick B, Hecht B, Wild UP: *Appl Phys Lett* 1999, **75**:160-162.
16. Lambelet P, Sayah A, Pfeffer M, Philipona C, Marquis-Weible F: *Appl Opt* 1998, **37**:7289-7292.
17. Vo-dinh T, Zhang Y: **Optical Nanosensors for Medicine and Health Effect Studies.** *Handbook of nanophysics: nanomedicine and nanorobotics* (in press).
18. Dhawan A, Muth JF, Leonard DN, Gerhold MD, Gleeson J, Vo-Dinh T, Russell PE: *J Vac Sci Technol, B: Microelectron Nanometer Struct* 2008, **26**:2168-2173.
19. Holland L: **Vacuum Deposition of Thin Films.** Wiley, New York; 1956.

doi:10.1007/s11671-010-9744-5
**Cite this article as:** Zhang *et al.*: Design and Fabrication of Fiber-Optic Nanoprobes for Optical Sensing. *Nanoscale Res Lett* 2011 **6**:18.

Focus Article

# Single-cell monitoring using fiberoptic nanosensors

Tuan Vo-Dinh* and Yan Zhang

This article is a review on the design, fabrication, and applications of fiberoptic nanosensors for *in vivo* monitoring of individual living cells. The nanosensors were fabricated with tapered optical fibers with distal ends having nanometer-sized diameters. Bioreceptors, such as antibody, peptides, and nucleic acids, are immobilized on the fiber tips and designed to be selective to target analyte molecules of interest. A laser beam is transmitted into the fiber, producing an evanescent field at the tip of the nanofiber that is used to excite target molecules bound to the bioreceptor molecules. The fluorescence originated from the analyte molecules is detected by a photo-detection system. The advantages and limitations of nanosensors in providing minimally invasive tools to probe subcellular compartments inside individual living cells for health effect studies and medical applications are discussed in detail.  *WIREs Nanomed Nanobiotechnol* 2011 3 79–85 DOI: 10.1002/wnan.112

## INTRODUCTION

Rapid progress in measurement technology has made it possible to characterize the intracellular components and understand the function of a single cell under heterogeneous environments. For instance, capillary electrophoresis (CE) can detect single cell compounds by electrochemistry and laser-induced fluorescence.[1] Matrix-assisted laser desorption/ionization mass spectrometry (MALDI-MS) has been used in detecting peptides and proteins from single cells.[2] Whole-cell sampling allows simultaneous detection of multiple species while sacrificing the spatial information. Cellular imaging based on Raman spectroscopy is powerful in visualizing the molecular composition of subcellular compartments without the need for labeling.[3] Atomic force microscopy (AFM) offers fascinating possibilities to resolve biological surface structures with molecular resolution on living cells.[4] Fiber optic nanosensor has achieved great success in sensing biotargets and molecular signaling processes inside single living cells with faster detection than Raman mapping.[5–21]

Fiberoptic nanosensors are suitable for sensing intracellular/intercellular physiological and biological parameters in submicron environments. Over the last two decades, our laboratory has been interested in the investigation and development of fiberoptic chemical sensors and biosensors for environmental and biochemical monitoring.[5–21] Initially the development of fibers with submicron distal diameters between 20 and 500 nm has led to advances in near-field scanning optical microscopy (NSOM).[22,23] Chemical nanosensors were developed for monitoring calcium and nitric oxide, among other physico-chemicals in single cells.[24,25] Nanobiosensors with antibody probes have been developed to detect biochemical targets inside single living cells.[11,13,15,18] Optical fibers having nanoscale tips were developed initially to serve as scanning probes in near-field optical microscopes.[23] The development of such a probe capable of obtaining measurements with a spatial subwavelength resolution was reported.[22] Due to its high spatial resolution (subwavelength), near-field microscopy has received great interest and has been used in many applications.[23] The combination of NSOM and Raman spectroscopy was used to achieve subwavelength 100-nm spatial resolution.[26,27] The silver-coated nanostructured substrates are capable to induce the plasmonic effect, which could enhance the Raman signal of the adsorbate molecules up to $10^8$ times.[28] Single-molecule detection and imaging schemes using nanofibers could open new capabilities in the investigation of the complex biochemical reactions and pathways in biological systems at the single cell level leading to important applications in medicine and health effect studies.

*Correspondence to: tuan.vodinh@duke.edu

Fitzpatrick Institute for Photonics, Departments of Biomedical Engineering and Chemistry, Duke University, Durham, NC, USA

DOI: 10.1002/wnan.112

  

# DEVELOPMENT OF OPTICAL NANOSENSORS FOR SINGLE-CELL MONITORING

## Fabrication of Fiberoptic Nanofibers

There are several methods for fabricating nanofibers. One method involves the laser pulling method, which consists of local heating of an optical fiber using a laser and subsequently pulling the fiber apart. Fabrication of nanosensors requires techniques capable of making reproducible optical fibers with submicron-sized diameter core. The laser pulling process is a time-dependent heating effect where laser power, timing of pulling, velocity setting, and pulling force are important parameters that contribute to the taper shape and tip size. Since transmission efficiency is highly dependent on the taper shape, it is crucial to control the tip shape in the fabrication of high-quality nanoprobes. Figure 1 illustrates the experimental procedures for the fabrication of nanofibers using the micropipette puller (Sutter Instruments P-2000).[18] A scanning electron microscopy (SEM) photograph of one of the fiber probes fabricated for studies is shown in Figure 2(a). The distal end of the nanofiber is approximately 40 nm.

The metallic coating process is an important step in nanoprobe fabrication. A thin film of an opaque metal such as aluminum, silver, or gold is coated along the outside walls of the tapered optical fiber tip to form an optical light pipe free of defects, which would permit photons to escape from the tapered sides of the optical fiber. An optical aperture to allow evanescent wave excitation is formed at the tip's apex by metal evaporation at an angle. Such a coating system is illustrated in Figure 3. An array of fiber probes is attached on a rotating motor installed inside a thermal evaporation chamber.[9,18,29] While the probes are rotated, the metal is allowed to evaporate onto the tapered side of the fiber tip to form a thin coating. The fiber is pointing away from the evaporation source with an angle of approximately 25°. The tapered end was coated with approximately 75–150 nm of metal in a thermal evaporator (Quorum Technologies E6700). With the metal coating, the size of the probe tip is approximately 200–350 nm. Figure 2(b) shows a gold-coated probe tip with a diameter about 350 nm. Due to the inclination angle, the distal ends of the fiber tips are shadowed from evaporation when the fiber tips are tilted away from the metal source. A nanoaperture, i.e., uncoated region at the distal end, was formed on the fiber tip that can be used for optical excitation and subsequent binding with bioreceptors. The size of the nanoaperture is determined by the angle between fiber axis and evaporation direction. The optimal angle of inclination can be determined

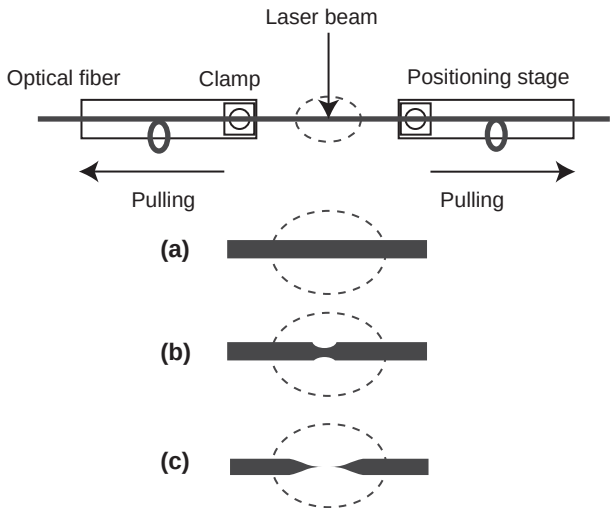


**FIGURE 1** | The fabrication of nanofibers through laser pulling. (a)–(c) The course of pull in time. In (c), a nanotip has been formed.

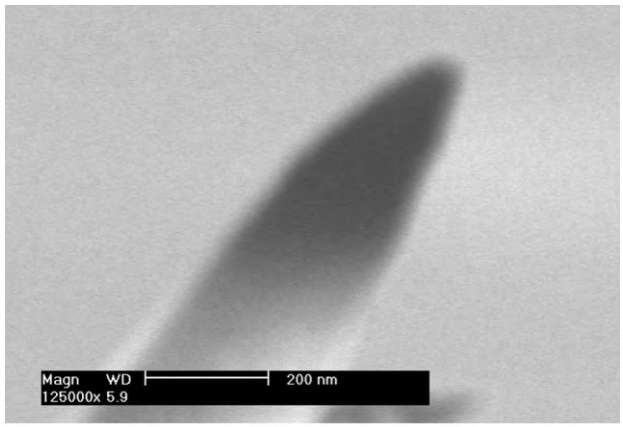


(a)

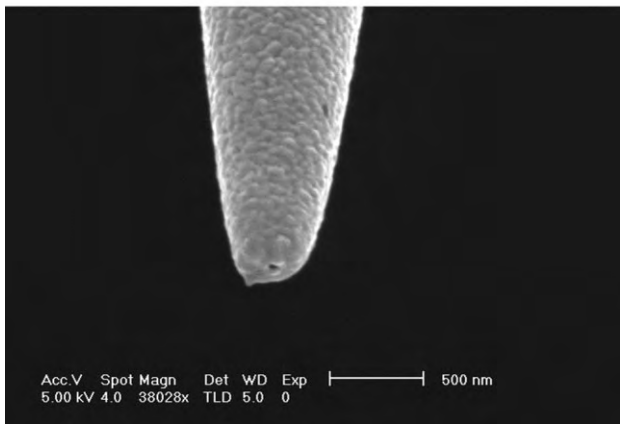


(b)

**FIGURE 2** | Scanning electron photograph of an uncoated nanofiber (a) and a gold-coated nanofiber (b).

  

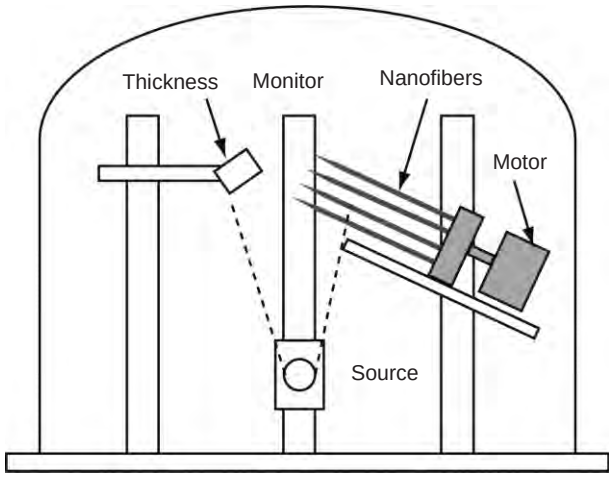


**FIGURE 3** | Angle evaporation of nanofibers in a thermal evaporator.

through characterization of nanoapertures under SEM. SEM measurements can analyze the actual size of the tip aperture. However, having a nanometer-sized aperture does not guarantee a good near-field probe. The tip aperture, even though it may appear small on the SEM, could be a result of aluminum over-coating, and hence not be a functional light aperture. Therefore, a functional scan is necessary to reveal the near-field effect from the probe and evaluate the effectiveness of the nanoprobe. NSOM enables functional analysis of the nanosensor probe by performing a scan on a standard sample, e.g., a Fischer pattern. The standard sample usually consists of patterns with size less than the diffraction limits ($0.5\lambda$) that can be determined by an AFM. The nanosensor probe was attached to an NSOM system working as an NSOM probe. Typically, the aperture of the probe roughly determines the resolution of the image. In other words, the image quality obtained with the fiber probe thus represents the quality of the probe.

The advantage of using gold instead of aluminum or silver is its higher melting temperature (660°C for Al, 960°C for Ag, and 1060°C for Au) and its better thermal resistance. The thermal stress generated during metallic film deposition damages the aperture due to the difference in thermal expansion coefficients of metal and quartz. Gold coating has the lowest thermal expansion coefficient ($23.1 \times 10^{-6}$/°C for Al, $18.9 \times 10^{-6}$/°C for Ag, $14.2 \times 10^{-6}$/°C for Au, $0.55 \times 10^{-6}$/°C for $SiO_2$), which will reduce the thermal destruction of the fiber tip. Furthermore, gold coatings are more stable in ambient conditions. The grain diameter is highly and sensitively dependent on the deposition pressure. Below $5 \times 10^{-6}$ torr, the size of the individual grains is smaller than 100 nm. There was a relationship between rate of metallic deposition and subsequent surface roughness, and studies revealed that a slower coating rate (<5 Å/second) resulted in better smoothness and the film opacity required for our intended sensor applications.

Traditional manufacturing processes still limit the quality of metal-coated fiber probes. Optical throughput of pulled nanoprobes is limited by the sharp taper angle. Another method of fabrication nanoprobes involves chemical etching. Chemical-etched tips have higher optical throughput; however, they do not usually have a flat distal end as the laser pulled ones. As discussed previously, it is difficult to form well-defined nanoapertures in shadow evaporation. Moreover, shadow evaporation often leads to either complete or irregular coated tips. Grainy structures of metal thin film could also increase the distance between the aperture and the sample, which reduces the resolution and intensity of the measurements. It is easy to form pin holes at the tapered region, which could lead to light leaking out of the fiber side walls. The aperture also deviates from ideal circular shape because of grains. A quantitative analysis of probe transmission efficiency becomes difficult. In spite of these challenges, nanofibers can be fabricated with good reproducibility by careful control of the experimental parameters during the fabrication process.

## Design of Nanobioprobes

The next step in the preparation of the nanobiosensor probes involves covalent immobilization of bioreceptor molecules such as antibodies and peptides onto the fiber tip. Silane modification techniques eliminate the nonspecific binding potential of silica for biomolecules. Modification of silica surface provides sites for coupling affinity ligands through covalent derivatization with a functional silane containing a functional group. Fiber nanoprobes were first silanized with 3-aminopropyltriethoxysilane (APTES), whereas carboxylic acid-functionalized probes were prepared by reaction of the amine functions with glutaric anhydride. N-hydroxysuccinimide (NHS) was used to modify a carboxyl group to an amine-reactive ester. This was accomplished by mixing NHS with a carboxyl-containing molecule and a dehydrating reagent 1-ethyl-3-[3-dimethylaminopropyl] carbodiimide hydrochloride (EDC). The addition of EDC induced a dehydration reaction between the carboxyl and the NHS hydroxyl group, giving rise to an NHS-ester-activated molecule. The NHS-ester-containing molecule was then reacted spontaneously with a primary amine groups present on the side chains of amino acids present in biomolecules. The reaction is much more efficient with NHS present because a stable intermediate is produced.

  

## DISCUSSION ON SINGLE-CELL MONITORING

### Detecting Fluorescent Biomarkers in Single Living Cells

Fiberoptic nanosensors are powerful tools for measurements in submicron environments and for probing individual chemical species in specific locations throughout a living cell due to their small nanoscale sizes. The experimental procedures for growing cell cultures for analysis using the nanosensors were described previously[9,18,30,31] and the optical measurement system used for monitoring single cells using the nanosensors is schematically illustrated in Figure 4. Traditional cell measurements usually use fluorescence microscopy, where fluorescent dye molecules were delivered into a cell and allowed to diffuse throughout. Depending upon the particular fluorescent dye molecules that were chosen, changes in the fluorescence properties of the dye could then be monitored using an imaging modality, as the dye came in contact with the analyte of interest. As this microscopy-based technique relies on imaging the fluorescent dyes, it requires the homogenous dispersion of the dye molecules through the various locations in the cell, which is limited by intracellular conditions (i.e., pH, etc.) or often does not even occur due to compartmentalization by the cell. Fiberoptic nanosensors provide an alternative cell monitoring modality that offers significant improvements over traditional methods, which are limited by the problems associated with cellular diffusion.

Nanosensors provide the appropriate tools for monitoring the transport of chemicals into cells, leading to improved understanding of the health effects associated with these species. Use of antibody-based nanoprobes to detect fluorescing chemicals inside a single cell has been demonstrated.[9,18,30,31] In a previous work,[18] the antibody probe was targeted against benzopyrene tetrol (BPT), an important biological compound, which was used as a biomarker of human exposure to the carcinogen benzo[a]pyrene (BaP), a polycyclic aromatic hydrocarbon of great environmental and toxicological interest because of its mutagenic/carcinogenic properties and its ubiquitous presence in the environment. Nanosensors have been developed for *in situ* measurements of the carcinogen BaP.[13] Detection of BaP transport inside single cells is of great biomedical interest as it can serve as a means for monitoring BaP exposure, which can lead to DNA damage.[32] To perform these measurements, polyclonal antibodies targeted to BaP were used as bioreceptors. The fluorescent BaP molecules are bound by interaction with the immobilized antibody receptor, forming a receptor–ligand complex. Following laser excitation of this complex, a fluorescence signal from BaP allows quantification of BaP concentration in the cell being monitored. The fluorescence method can achieve high sensitivity of detection. The intracellular measurements of BaP depend on the antibody–antigen reaction times involved. The success of single-cell measurements depends on several factors, including the sensitivity of the measurement system, the selectivity of the probe, and the small size of the nanofiber probes because the sizes of individual cells are generally small (1–10 μm). The small size of the probe allowed manipulation of the nanosensor at specific locations within the cells. Figure 5 depicts a fiberoptic nanoprobe inserted into a single cell.[24]

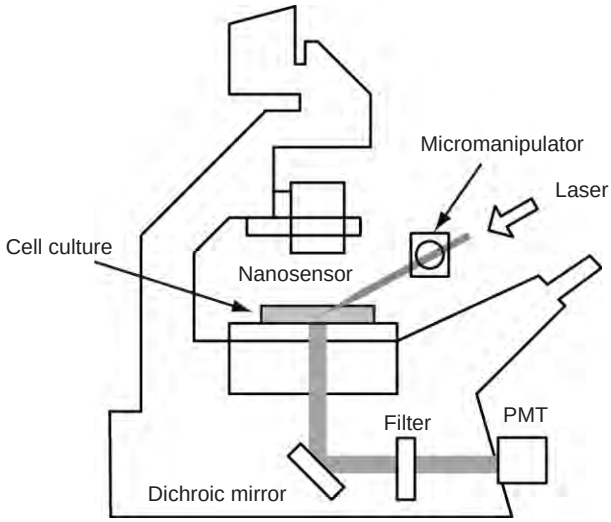


**FIGURE 4** | Instrumental system for fluorescence measurements of single cells using nanosensors.

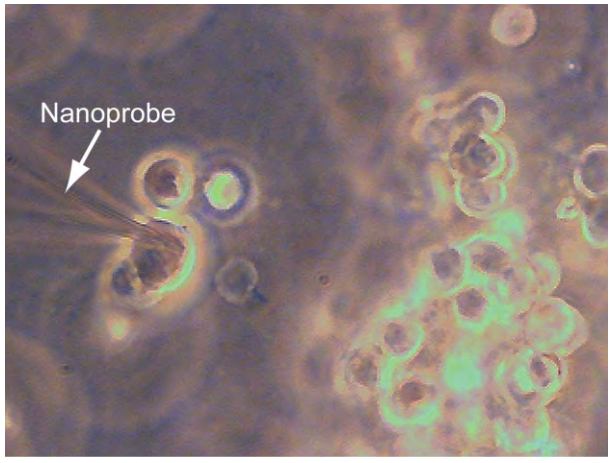


**FIGURE 5** | Picture of a fiberoptic nanoprobe inserted into a single cell.

In another study, nanosensors were developed and used for the measurement of intracellular concentrations of BPT in the cytoplasm of two different cell lines: (1) human mammary carcinoma cells and (2) rat liver epithelial cells, following treatment of the culturing media with an excess of BPT. The measurements were performed on rat liver epithelial cells (Clone 9) used as the model cell system. The cells were first incubated with BPT prior to measurements using the experimental procedures described previously.[18] Detection of BPT in single cells was then performed using antibody nanoprobes for excitation and a photometric system for fluorescence signal detection. The results demonstrated the possibility of *in situ* measurements of BPT inside a single cell. We have performed calibration measurements of solutions containing different BPT concentrations ranging from $1.56 \times 10^{-10}$ to $1.56 \times 10^{-8}$ M in order to obtain a quantitative estimation of the amount of BPT molecules detected. By plotting the increase in fluorescence from one concentration to the next versus the concentration of BPT, and fitting these data with an exponential function in order to simulate a saturated condition, a concentration of $(9.6 \pm 0.2) \times 10^{-11}$ M has been determined for BPT in the individual cell investigated.[9,18,30,31,33] In this study, the nanosensors used single-use bioprobes because the probes were used to obtain only one measurement at a specific time and could not be reused due to the strong association constant of the antibody–antigen binding process. The antibody probes, however, could be regenerated using ultrasound methods. Our laboratory has successfully developed a method using ultrasound to non-invasively release antigen molecules from the antibodies, and, therefore, to regenerate antibody-based biosensors.[34] The ultrasound regeneration scheme is a nondestructive approach that has the potential to be applied to *in situ* monitoring systems. The application of antibody-based nanoprobe was also limited by its nonspecific binding and inability to directly detect compounds without fluorescent labeling. Although this article is focused on nanoprobes using fluorescence detection, surface-enhanced Raman scattering (SERS) nanoprobes offer a promising alternative that can provide additional chemical structure information to identify intracellular species and physiological parameters in single living cells.[14]

## Monitoring of Apoptotic Pathways in Single Cells

Evaluation of the effectiveness of anticancer drugs such as the onset of apoptosis in living cells is an important process in drug development and therapy assessment. The cell death process known as apoptosis is executed in a highly organized fashion, indicating the presence of well-defined molecular pathways. Caspase activation is a hallmark of apoptosis, and probably one of the earlier markers that signals the apoptotic cascade.[35–37] These cysteine proteases are activated during apoptosis in a self-amplifying cascade. Experimental evidence suggests that caspase activation is essential for the apoptotic process to take place, although not all cell death is dependent upon caspase activation. Caspases have an essential role both in the initial signaling events of apoptosis, as well as in the downstream processes which produce the various hallmark signs of apoptosis. Activation of caspases such as caspases 2, 8, 9, and 10 leads to proteolytic activation of 'downstream' caspases such as 3, 6, and 7.

Nanobiosensors have been developed for monitoring the onset of the mitochondrial pathway of apoptosis in a single living cell by detecting enzymatic activities of caspase-9.[10] Minimally invasive analysis of single live MCF-7 cells for caspase-9 activity was demonstrated using a fiberoptic nanosensor which used a modified immunochemical assay format of a non-fluorescent enzyme substrate, leucine-glutamic acid-histidine-aspartic acid-7-amino-4-methyl coumarin (LEHD-AMC). LEHD-AMC covalently attached on the tip of an optical nanobiosensor was cleaved during apoptosis by caspase-9, thus generating free AMC molecules that become fluorescent upon laser excitation. An evanescent field was used to excite cleaved AMC and the resulting fluorescence signal was detected. By quantitatively monitoring the changes in fluorescence signals, caspase-9 activity within a single living MCF-7 cell was detected. Photodynamic therapy (PDT) protocols using the pro-drug $\delta$-aminolevulinic acid (ALA) were used to induce apoptosis in MCF-7 cells. The substrate LEHD-AMC was cleaved by caspase-9 and the released AMC molecules were excited and emitted a fluorescence signal (Figure 6). By

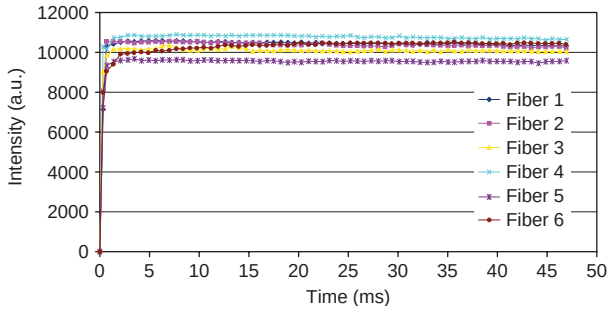


**FIGURE 6** | Detection of caspase-9 activity performed with nanosensors inserted into single live MCF-7 cells.

comparison of the fluorescence signals from apoptotic cells, induced by PDT treatment, and non-apoptotic cells, we successfully detected caspase-9 activity, which indicates the onset of apoptosis in the cells. The results show that the fluorescence signals obtained from the cells that were both incubated with ALA and photoactivated by laser excitation were much higher than the signal obtained from control groups, i.e., without laser activation.[10] The presence and detection of cleaved AMC in single live MCF-7 cells as a result of these experiments reflects the presence of caspase-9 activity and the occurrence of apoptosis. These results indicate that apoptosis can be monitored *in vivo* in a single living cell using optical nanobiosensors.

## CONCLUSION

Fiberoptic nanosensors for monitoring single cells have opened up new applications in molecular biology and medical diagnostics. Due to their small sizes, nanosensor provides important tools for minimal invasive analysis at single cellular or subcellular level. These nanotools can be used to study intracellular signaling processes and to investigate gene expression inside single living cells. Probing subcellular architecture and dynamic processes is essential in understanding the fundamental biological processes such as cell signaling pathways in a systems biology approach. Single-cell monitoring is also important in studies where the amount of cells obtained is limited, which could not be analyzed with other techniques. While fiberoptic nanoprobe is not ready for clinical use yet, there is no doubt that the current development of the fiberoptic nanoprobe technology will allow the quantitative analysis of chemical species involving cellular pathways and communications. By combining the nanoprobe technology with SERS-based detection, multiplexed analysis of multiple biomarkers and physical conditions will be possible. Other optical methods such as surface plasmon resonance (SPR) and interferometry can also be integrated with fiberoptic nanoprobes, thus increasing their versatility. Fiberoptic nanoprobe will provide unprecedented details in single cell analysis leading to a better fundamental understanding of cellular biology and more translational applications in medicine and health effect studies.

## ACKNOWLEDGEMENTS

The author acknowledges the contribution of G.D. Griffin, J.P. Alarie, B.M. Cullum, and P. Kasili. This research is sponsored by the National Institutes of Health (1R01ES014774 and R01-EB006201) and US Army Medical Research and Material Command (W81XWH-09-1-0064).

## REFERENCES

1. Munce NR, Li JZ, Herman PR, Lilge L. Microfabricated system for parallel single-cell capillary electrophoresis. *Anal Chem* 2004, 76:4983–4989.
2. Rubakhin SS, Greenough WT, Sweedler JV. Spatial profiling with MALDI MS: Distribution of neuropeptides within single neurons. *Anal Chem* 2003, 75:5374–5380.
3. van Manen HJ, Kraan YM, Roos D, Otto C. Single-cell Raman and fluorescence microscopy reveal the association of lipid bodies with phagosomes in leukocytes. *Proc Natl Acad Sci USA* 2005, 102:10159–10164.
4. Hinterdorfer P, Dufrene YF. Detection and localization of single molecular recognition events using atomic force microscopy. *Nat Methods* 2006, 3:347–355.
5. Alarie JP, Bowyer JR, Sepaniak MJ, Hoyt AM, Vodinh T. Fluorescence monitoring of a benzo[a]pyrene metabolite using a regenerable immunochemical-based fiberoptic sensor. *Anal Chim Acta* 1990, 236:237–244.
6. Alarie JP, Vo-Dinh T. A fiberoptic cyclodextrin-based sensor. *Talanta* 1991, 38:529–534.
7. Alarie JP, Vo-Dinh T. Antibody-based submicron biosensor for benzo[a]pyrene DNA adduct. *Polycyclic Aromat Compd* 1996, 8:45–52.
8. Cullum BM, Griffin GD, Miller GH, Vo-Dinh T. Intracellular measurements in mammary carcinoma cells using fiber-optic nanosensors. *Anal Biochem* 2000, 277:25–32.
9. Cullum BM, Vo-Dinh T. The development of optical nanosensors for biological measurements. *Trends Biotechnol* 2000, 18:388–393.
10. Kasili PM, Song JM, Vo-Dinh T. Optical sensor for the detection of caspase-9 activity in a single cell. *J Am Chem Soc* 2004, 126:2799–2806.
11. Kasili PM, Vo-Dinh T. Detection of polycyclic aromatic compounds in single living cells using optical nanoprobes. *Polycyclic Aromat Compd* 2004, 24:221–235.
12. Kasili PM, Vo-Dinh T. Optical nanobiosensor for monitoring an apoptotic signaling process in a single living

  

cell following photodynamic therapy. *J Nanosci Nanotechnol* 2005, 5:2057–2062.

13. Kasili RM, Cullum BM, Griffin GD, Vo-Dinh T. Nanosensor for in vivo measurement of the carcinogen benzo[a]pyrene in a single cell. *J Nanosci Nanotechnol* 2002, 2:653–658.
14. Scaffidi JP, Gregas MK, Seewaldt V, Vo-Dinh T. SERS-based plasmonic nanobiosensing in single living cells. *Anal Bioanal Chem* 2009, 393:1135–1141.
15. Song JM, Kasili PM, Griffin GD, Vo-Dinh T. Detection of cytochrome c in a single cell using an optical nanobiosensor. *Anal Chem* 2004, 76:2591–2594.
16. Tromberg BJ, Sepaniak MJ, Alarie JP, Tuan VD, Santella RM. Development of antibody-based fiber-optic sensors for detection of a benzo[a]pyrene metabolite. *Anal Chem* 1988, 60:1901–1908.
17. Vo-Dinh T. Nanosensing at the single cell level. *Spectrochim Acta Part B* 2008, 63:95–103.
18. Vo-Dinh T, Alarie JP, Cullum BM, Griffin GD. Antibody-based nanoprobe for measurement of a fluorescent analyte in a single cell. *Nat Biotechnol* 2000, 18:764–767.
19. Vo-Dinh T, Kasili P. Fiber-optic nanosensors for single-cell monitoring. *Anal Bioanal Chem* 2005, 382:918–925.
20. Vo-Dinh T, Kasili P, Wabuyele M. Nanoprobes and nanobiosensors for monitoring and imaging individual living cells. *Nanomedicine* 2006, 2:22–30.
21. Vo-Dinh T, Tromberg BJ, Griffin GD, Ambrose KR, Sepaniak MJ, Gardenhire EM. Antibody-based fiberoptics biosensor for the carcinogen benzo(a)pyrene. *Appl Spectrosc* 1987, 41:735–738.
22. Betzig E, Chichester RJ. Single molecules observed by near-field scanning optical microscopy. *Science* 1993, 262:1422–1425.
23. Pohl DW. In: Sheppard CJR, Mulevy T, eds. *Advances in Optical and Electron Microscopy*. London: Academic; 1991, 243–312.
24. Tan WH, Shi ZY, Kopelman R. Development of submicron chemical fiber optic sensors. *Anal Chem* 1992, 64:2985–2990.
25. Tan WH, Shi ZY, Smith S, Birnbaum D, Kopelman R. Submicrometer intracellular chemical optical fiber sensors. *Science* 1992, 258:778–781.
26. Deckert V, Zeisel D, Zenobi R, Vo-Dinh T. Near-field surface enhanced Raman imaging of dye-labeled DNA with 100-nm resolution. *Anal Chem* 1998, 70:2646–2650.
27. Zeisel D, Deckert V, Zenobi R, Vo-Dinh T. Near-field surface-enhanced Raman spectroscopy of dye molecules adsorbed on silver island films. *Chem Phys Lett* 1998, 283:381–385.
28. Vo-Dinh T. Surface-enhanced Raman spectroscopy using metallic nanostructures. *Trends Anal Chem* 1998, 17:557–582.
29. Vo-Dinh T, Sepaniak MJ, Griffin GD, Alarie JP. Immunosensors: principles and applications. *Immunomethods* 1993, 3:85–92.
30. Vo-Dinh T, Cullum B. Biosensors and biochips: advances in biological and medical diagnostics. *Fresenius' J Anal Chem* 2000, 366:540–551.
31. Vo-Dinh T, Cullum BM, Stokes DL. Nanosensors and biochips: frontiers in biomolecular diagnostics. *Sens Actuators B* 2001, 74:2–11.
32. Vo-Dinh T. *Chemical Analysis of Polycyclic Aromatic Compounds*. New York: John Wiley & Sons; 1989.
33. Vo-Dinh T, Griffin GD, Alarie JP, Cullum BM, Sumpter B, Noid DJ. Development of nanosensors and bioprobes. *J Nanoparticle Res* 2000, 2:17–27.
34. Moreno-Bondi MC, Mobley J, Alarie JP, Vo-Dinh T. Antibody-based biosensor for breast cancer with ultrasonic regeneration. *J Biomed Opt* 2000, 5:350–354.
35. Hengartner MO. Apoptosis—DNA destroyers. *Nature* 2001, 412:27–29.
36. Ricci JE, Gottlieb RA, Green DR. Caspase-mediated loss of mitochondrial function and generation of reactive oxygen species during apoptosis. *J Cell Biol* 2003, 160:65–75.
37. Wolf BB, Green DR. Suicidal tendencies: apoptotic cell death by caspase family proteinases. *J Biol Chem* 1999, 274:20049–20052.

  